Adaptive Analysis Of The Secondary Path For Active Noise Control

Audio Engineer Project Report

Andrés
Ureta Staackmann

Supervision: DI Markus Guldenschuh

Graz, July 26, 2013

institut für elektronische musik und akustik

Abstract

Headphones with ANC (Active Noise Control) have at least one microphone for each side, left and right respectively, delivering information about the undesired signal to be eliminated. An anti-noise signal can be generated (with an inversion of the disturbing signal's phase) in order to inhibit as much as possible the disturbing signal. From the superposition law, it follows a cancellation of the disturbing signal by means of summation of both the latter and the anti-noise signal generated by the adaptive filter. The whole system is controlled by the LMS algorithm that will adapt the filter coefficients according to the disturbing signal and its incidence angle amongst others.

This algorithm may require, depending on the structure used, different reference signals. The reference signal describing the disturbing signal can be provided by two additional external microphones, one for each side. This signal can also be estimated in case no external microphones are available. The reference error signal provided by the inner microphones is on the other hand absolutely necessary in order to have feedback about the residual noise, i.e. the remains of the disturbing signal after the noise cancellation process. These reference signals must possess the same phase (time displacement) in order for the algorithm to work properly. They must hence be delayed according to the latency of the system which is the time needed for the AD and DA conversions, respectively. Also the transmission path between the loudspeaker and the listener's ear, the so called secondary path, will vary every time the listener puts on the headphones and with it the group delay as well. Compensating the influence of the secondary path represents another challenge for ANC systems. Therefore it is necessary to artificially delay the reference signals corresponding to the given situation. Whereas the latency of a system does not change over time, the group delay of the secondary path may constantly vary affecting directly the system's performance.

In this project, the effects of a constant changing secondary path as well as the estimation accurateness needed for it on a ANC system are to be studied. Moreover an adaptive identification method of the secondary path is to be developed. In addition to the known adaptive methods for a secondary path analysis, a new approach relying on a data base of measured secondary paths is to be implemented.

Contents

1 Introduction

1.1 Topic and Motivation

Active Noise Control (ANC) rests upon the superposition principle. This one states that the net response at a given place and time caused by two or more stimuli is the sum of the responses which would have been caused by each stimulus individually. Eq. 1 puts down this law in a mathematical way

$$F(x_1 + x_2 + \ \ldots \ + x_n) = F(x_1) + F(x_2) + \ \ldots \ + F(x_n). \tag{1}$$

The idea behind ANC is to generate an anti-signal that results, when added to the disturbing signal considered, in a destructive interference of both signals at the sensor position. Depending on the nature of the disturbing signal and the capacity of the algorithm, amongst other things, is a total (ideally) or a partial cancellation of the disturbing signal possible. The latter represents the more realistic scenario and is going to be the subject of study in a subsequent section. A reference signal describing the residual error from the cancelling process is absolutely necessary for the algorithm to work. A second reference signal describing the disturbing signal, i.e. the signal to be cancelled, is needed depending on the algorithm's structure being used (see Section 2).

The adaptive filter is controlled by the $NFxLMS$ algorithm. This is a LMS algorithm where the input signal is filtered and an additional normalisation of the step size is carried out. Detailed reports concerning ANC can be found in [KM99] and [ZLS01].

1.2 Purpose

The main problems concerning the realisation of such a system are

1. the temporal basis of the reference signals and
2. the group delay of the secondary path.

The first one depends on the AD and DA conversion times [1] of the system. This parameter is constant for a given system and will from now on be called $latency$. On the other hand, the group delay [2] of the secondary path will vary every time the listener puts on the headphones.

1. Analog-to-Digital and Digital-to-Analog converters are necessary in order to convert a physical to an electric signal and vice versa.

2. This is a measure for the time delay of the amplitude envelopes of a signal as a function of frequency.

Definition. The secondary path is the transmision path from the loudspeaker to the ear. This acoustical path is obtained by measurements using the so called error microphone inside the ear cushions.

Considering the secondary path's absolute value and phase will be enough in order to describe it. Both the secondary path S and its estimation $\hat{S}$ can be fully characterised by Eq. 2. The circumflex accent is used throughout this study to denote an estimation of a given variable or parameter. [3]

$$\begin{aligned} S =& |S| \cdot e^{i\theta} \\ \hat{S} =& |\hat{S}| \cdot e^{i\hat{\theta}} \end{aligned} \tag{2}$$

The focus of this work is to study the effects on ANC when implementing different secondary paths and their estimations. A special emphasis is made concerning the accuracy needed for the estimation of the secondary path in order for the algorithm to work properly. This analysis constitutes an important part of the study presented here and should result in answering whether or not Eq. 3 has to hold in order to guarantee the algorithm's sability when cancelling broad band noise signals.

In addition, a new identification method of the secondary path is to be conceived. Identifying the secondary path is considered to be necessary if the algorithm's stability depends on it. The new approach should at the same time lean on a data base of measured secondary paths.

$$S = \hat{S} \tag{3}$$

1.3 Structure

This work is devided in sections. A brief introduction to several topics of importance is given in Section 2. An overview of the algortihm used as well as the different structures for its implementation is also given. Finally, the main idea for an online identification of the secondary path is presented.

The simulations concerning the stability criteria for both structures considered are presented in Section 3. Further, the influence of the step size on the algorithm's performance is also studied. Starting point for these considerations is the latency which will vary from system to system. The simulations in this section reflect the system as well as the measured secondary paths that were available at that time.

The measurement realised for this study is described in detail in Section 4. Its results are the foundation for the identification method of the secondary path presented in Section 5. The conclusion with a summary of the results obtained in this study and a perspective of the method's application are comprised in Section 6.

3. The notation S_{hat} can also be found in some figures when referring to $\hat{S}$.

2 Basic Principles

2.1 Normalised FxLMS Algorithm

The algorithm used to control the adaptive filter is a modification of the LMS (Least Mean Square) algorithm [4]. This adaptive algorithm uses a gradient based method of the steepest decent with the goal of minimising the cost function, i.e. the squared error signal. It incorporates an iterative process that makes successive corrections of the weight vector in direction of the negative gradient vector of the cost function, while using estimations of it from the available data. The process will eventually lead to the minimum square error without requiring the calculation of the correlation function nor matrix inversions. [5] The $FxLMS$ algorithm is given by

$$\mathbf{w}[n] = \mathbf{w}[n-1] + \mu \cdot e[n] \cdot \mathbf{x}_f[n], \tag{4}$$

where μ is the step size parameter, e[n] is the residual noise signal picked up by the error microphone and $\mathbf{x}_f[n]$ is the filtered reference signal vector. Following the concept of the normalised LMS algorithm, see also [Dou94], the $NFxLMS$ is defined by

$$\mathbf{w}[n] = \mathbf{w}[n-1] + \mu[n] \cdot e[n] \cdot \mathbf{x}_f[n], \tag{5}$$

where the normalised time-varying step size parameter $\mu[n]$ becomes a function of n and is given by

$$\mu[n] = \frac{\tilde{\mu}}{\|\mathbf{x}_f[n]\|_2^2 + \beta}. \tag{6}$$

$\tilde{\mu}$ is the fixed step size parameter, $\|\mathbf{x}_f[n]\|_2$ is the $l_2 - norm$ of the filtered reference signal vector and β is a small positive number added to avoid divison by zero. More information concerning this algorithm can be found in [AM10] and [LP02].

In order to distinguish scalars from vectors, a bold notation is used for multidimensional elements. Matrices are presented in capital letters and using a bold face as well.

The Secondary Path and the Filtered-x LMS Algorithm. As depicted in Fig. 1 and Fig. 2, the secondary path S is a part of the transmission path and must therefore be compensated in order for the algorithm to remain stable and work properly. The main problem lies in the time alignment between the error signal $e[n]$ and both reference signals $x[n]$ and $\hat{x}[n]$. Morgan in [Mor80] suggested two approaches in order to solve this problem.

4. Algorithm introduced by Widrow and Hoff in 1959. For further information please refer to [WH60].
5. This is the case under assumption that the algorithm remains stable and that the negative gradient can be found.

The first solution consists in placing an inverse filter $S^{-1}(z)$ in series with $S(z)$ to remove its effect. Since an inverse filter does not necessarely exist nor is easy to compute, the second solution is favoured. This one suggests the placement of an identical filter, in this case an estimation $\hat{S}(z)$ of the secondary path $S(z)$, in the reference signal path of the weight update for the LMS algorithm. Filtering the reference signal results in the so-called Filtered-x LMS (abbreviated FxLMS) algorithm.

Inculding the normalisation of the step size done in Eq. 6 will yield the NFxLMS algorithm used throughout the simulations and work presented in this study. An accurate modelling of the secondary path or a better convergence of the algorithm are some of the aspects studied in the wide research done for this algorithm. For more information concerning these two aspects can be found in [RS96] and [AAK04] amongst others.

2.2 Algorithm's Structures

2.2.1 Feedforward

A total of four microphones[6] are needed when implementing the $Feedforward$ structure depicted in Fig. 1. These microphones are responsable for delivering the reference signals used by the algorithm. The external ones supply the noise signal to be cancelled, i.e. the disturbing signal, while the inner microphones provide the error signal used by the LMS algorithm. The error signal $e[n]$ describes the residual noise that remains after the noise cancellation process.

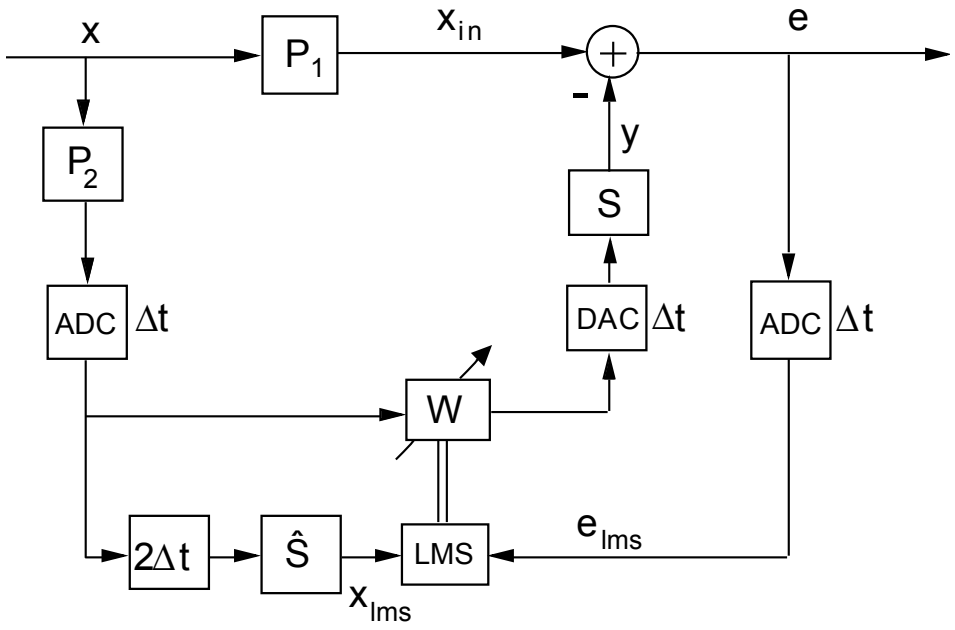

Figure 1: Feedforward structure.

6. Two for each side and placed one outside and the other inside the ear cuchions, respectively.

The transfer functions $P1$ and $P2$ depicted in Fig. 1 and Fig. 2 represent transfer functions describing the measurements of the reference signals by the microphones. $P1$ describes for instance the low-pass characteristic of the ear cushions while $P2$ simulates the measurement of the disturbing signal on the external surface of the headphones.

The two AD conversion units represent the two converting units responsible for the digitalisation of the acoustic signals. The DA conversion unit is to be interpreted as the reproduction point, i.e. the headphone's loudspeaker membrane itself. The latency of the system is compensated by the delay unit built in the lower path of the structure. Its output is the delayed and filtered reference signal with the adequate time basis for the LMS algorithm. Together with the delayed error signal $e_{LMS}[n]$, are both reference signals provided for the algorithm to compute the adaptive filter coefficient weights $\mathbf{w}[n]$. A special feature of this structure is the fact that the estimation of the secondary path $\hat{S}$ is applied one time only. As shown in Section 3, this factor will be decisive.

2.2.2 Feedback

The main difference between the $Feedback$ and the $Feedforward$ structures is the way the reference signal, describing the disturbing signal, is obtained. In this case, $\hat{x}_{in}[n]$ is estimated and not measured (as done with the $Feedforward$ structure) resulting in a reduction of the total number of microphones needed from four to two. Thus the reference signal is obtained by adding the estimation of the adaptive filter output $\hat{y}[n]$ and the delayed signal $e_{LMS}[n]$ picked up by the error microphone.

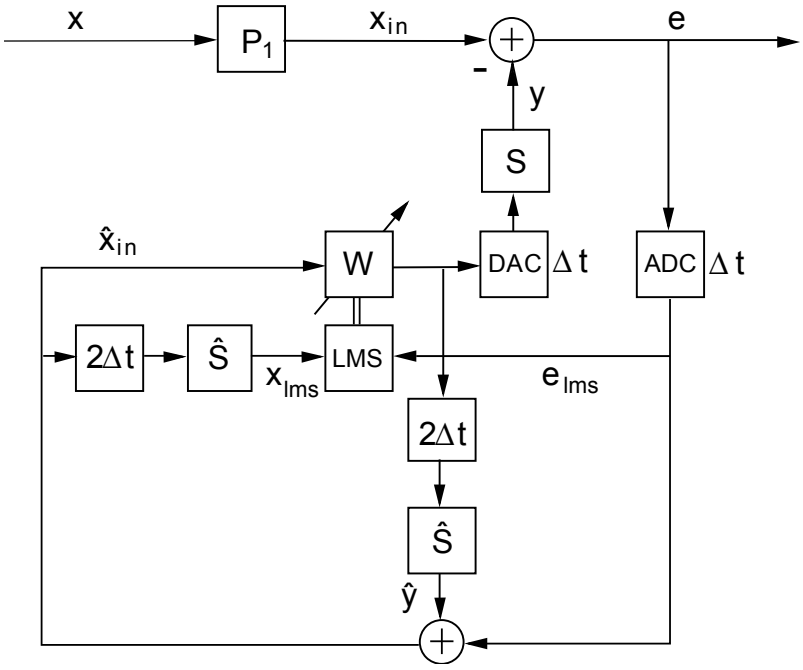

Figure 2: Feedback structure.

The estimated secondary path $\hat{S}$ is required up to two times for the $Feedback$ structure illustrated in Fig. 2. As mentioned earlier in this section, $\hat{S}$ is apllied in order to remove the influence of the secondary path S. For this structure, it is also needed for computing the estimated anti-noise signal $\hat{y}[n]$. Eq. 7 outlines the estimation process of the disturbing signal $\hat{x}_{in}[n]$ for this particular structure of the LMS algorithm.

$$\hat{x}_{in}[n] = \hat{y}[n] + e[n] \tag{7}$$

As shown in future sections, this fact will be of extreme importance when analysing the influence of $\hat{S}$ on the algorithm's performance. Epecially when Eq. 3 is not valid, i.e. answering to a more realistic scenario, where S cannot be fully modelled by $\hat{S}$.

2.3 Attenuation by the Ear Cushions

The attenuation that results from the ear cushions was also included in the simulations in an attempt of making them as genuine as possible. The low-pass characteristic of the attenuation is depcited in Fig. 3. At first the red curve was implemented but resulted in an unwanted attenuation for lower frequencies. This can be explained by the loudspeakers used for that measurement, which did not reproduce low frequencies with enough power to actually describe the real low-pass characteristic that is introduced by the ear cushions.

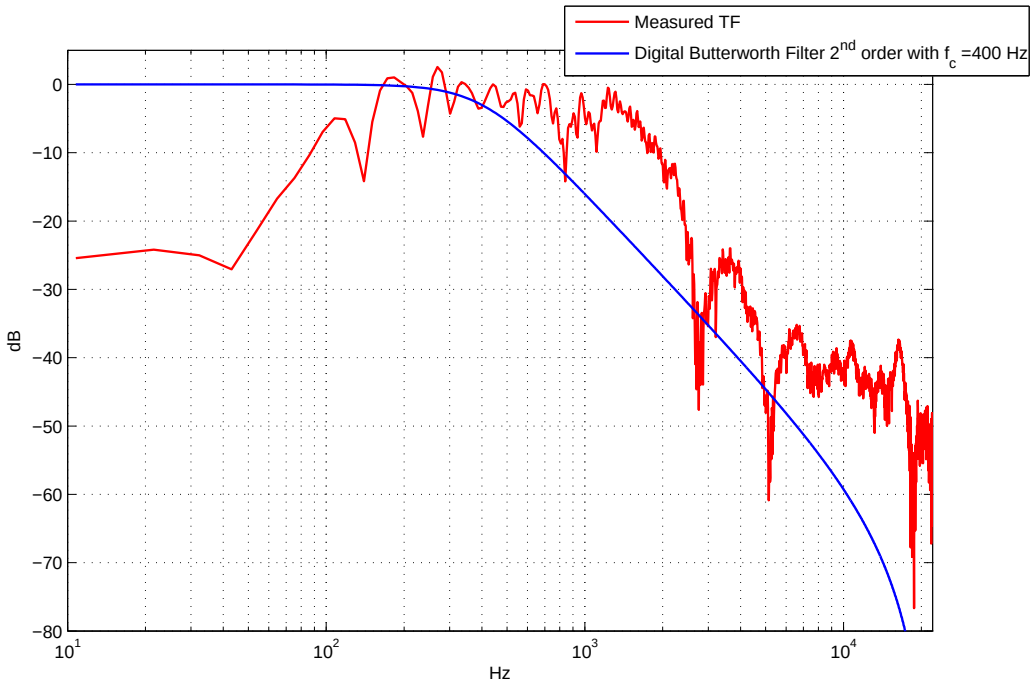

Figure 3: Lowpass filter characteristics of the attenuation by the ear cushions.

Its more or less band-pass characteristic becomes evident when comparing it to the blue curve. The latter was generated in Matlab by a digital $Butterworth$ filter 2^{nd} order with a cut-off frequency of $400Hz$. The amplitude falls from this frequency on with $-40dB$ per decade resulting in the wanted low-pass characteristic. The digitally generated curve was thus applied as $P1$ for both structures and for all simulations that followed (see Section 3).

2.4 Online Secondary Path Identification

Being able to identify the secondary path S is relevant only if Eq. 3 has to hold in order for the algorithm to work properly. A significant improvement of the algorithm's performance would also justify the necessity of an online secondary path identification. It is therefore important to analyse both structure's stability criteria as well as the influence of the estimated secondary path $\hat{S}$ on the algorithm's performance.

The range of the step size μ, for which the algortihm's stability is guaranteed, while producing a good anit-noise signal as well as the influence of the system's latency are some of the aspects that need to be studied. In addition, the group delay introduced by S and the repercussions of an inaccurate compensation of it shall also be evaluated.

Identification Method. The main idea is to leak a $15Hz$ sinusoidal signal when the listener is using the headphones in order to find out the manner in which these are being worn, i.e. a rather leak-proof or leaky manner. An exact measurement of the secondary path is not necessary nor desired since it would require the use of a measurement signal such as an exponential sweep or white noise [7]. Using one of these signals would disturb the listening experience. Hence a sinusoidal test signal with an inaudible frequency [8] is chosen.

As shown in Section 5, the distinction between two manners of wearing the headphones, i.e. a leak-proof and a leaky manner, will be enough for the online secondary path identification. The goal is to know if the headphones are worn in a rather leak-proof or leaky manner. This will be done by comparing both the test and the error signals. The latter is delivered for each channel by its inner microphone. How this is accomplished should not be of interest at this stage. Knowing on the other hand, to what extent it is necessary to accurately estimate the secondary path is relevant and constitutes the main issue treated in the next section.

7. Random signal with a constant power spectral density meaning it contains equal power within a desired frequency band.

8. The test frequency is placed at $15Hz$ beacuse frequencies at this bandwidth are not audible for humans and subsequently do not disturb the listening experience.

3 Simulations

Different secondary paths were available for the simulations presented in this section. These were measured within the work of Guldenschuh in [Gul12] at the IEM [9] and are the basis of the analysis and conclusions done here. Some of them represent extreme cases that will not occur under normal circumstances.

The many scenarios were realised by putting the ANC headphones in different manners [10] on the dummy head, see also Fig. 19, for then measuring the secondary paths. As seen in Fig. 4, the whole spectrum covers many cases between a leak-proof and a leaky manner of wearing the headphones.

The transfer functions show important fluctuations, especially for lower frequencies. It is exactly in this frequency range where through measurements it becomes possible to identify the manner in which the headphones are being worn by the listener. The last transfer function depicted in Fig. 4, i.e. $TF_{unclosed}$, will not be considered given the enormous difference in amplitude levels between it and all the others, but mainly because holding the headphones entirely appart from the dummy head does not represent a real scenario when an air leakage is given.

How big is the error signal when Eq. 3 does not hold or how accurate is it necessary to estimate the secondary path so that the algorithm's stability is guaranteed are the main questions to answer at this stage.

Referenced Error Signal. The different scenarios simulated in this section are compared to each other by analysing their referenced error signals. These are defined as the ratio of the cumulative sum of both the error signal $e[n]$ and the disturbing signal $x[n]$. The first one is obtained by simulating the noise cancelling process for the considered secondary paths illustrated in Fig. 4. This relationship is described by Eq. 8 where e_{ref} is the referenced squared error signal and m the length of both signals with $k = 0, \cdots, m$.

$$e_{ref}[k] = \frac{\sum_{n=0}^{k} e^2[n]}{\sum_{n=0}^{k} x^2[n]} \tag{8}$$

9. Institut für Elektronische Musik und Akustik Graz, AT.
10. These vary from keeping the headphones from the dummy head at different distances to tying them with a rope. Metallic tubes were also introduced between the headphones and the dummy head for simulating an air leackage.

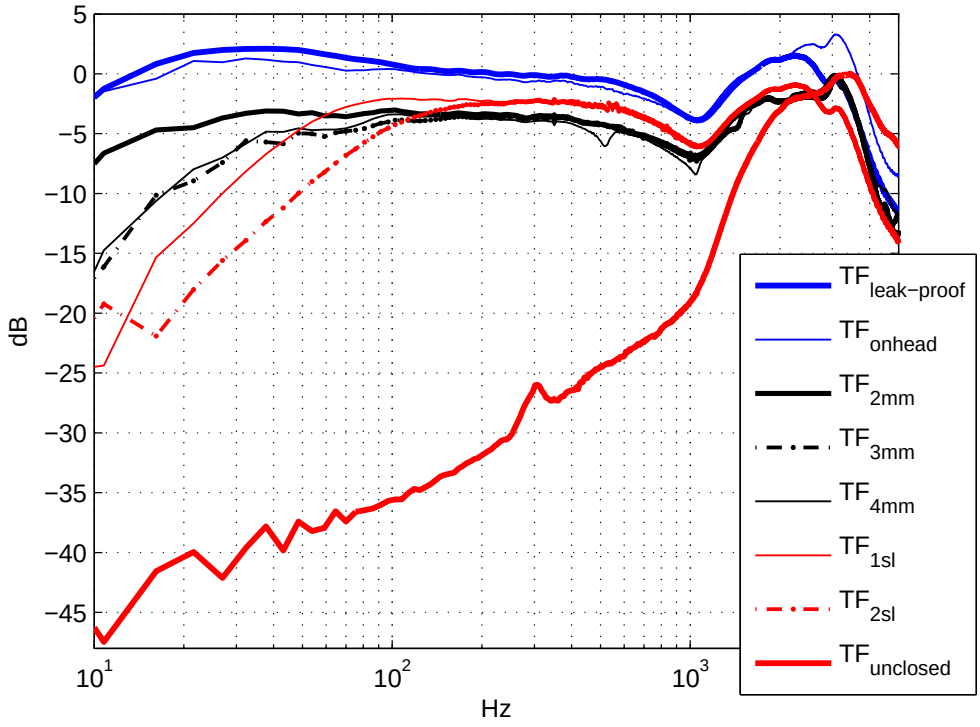

Figure 4: Secondary paths provided for a first analysis.

3.1 High Latencies

The system that was available at first had a latency of 21ms. A simulation with broadband noise was therefore not meaningful. Thus a disturbing signal consisting on three sinusoidal components was chosen. The frequencies were randomly chosen such that they would not form a harmonic multiple. Depicted in Fig. 5 is its spectrum where the sinusoidal components at $46Hz$, $1160Hz$ and $5560Hz$, respectively are visible. Sensor noise was also added at the microphone positions, see Fig. 1 and Fig.2, in order to make the simulations more realistic.

3.1.1 Feedforward Structure

It is assumed that Eq. 3 does not hold while reducing the length of the estimated secondary path at the same time. The simulation was done for $\hat{S} = TF_{leak-proof}$ and $S = TF_{1sl}$. This means that it is wrongly assumed that the listener wears the headphones in a leak-proof manner. Depicted in Fig. 6 are the referenced squared error signals with a progressive reduction of the estimated secondary path's length. The step size μ was set at 0.001 in an attempt to show the influence of the estimated secondary path's length only.

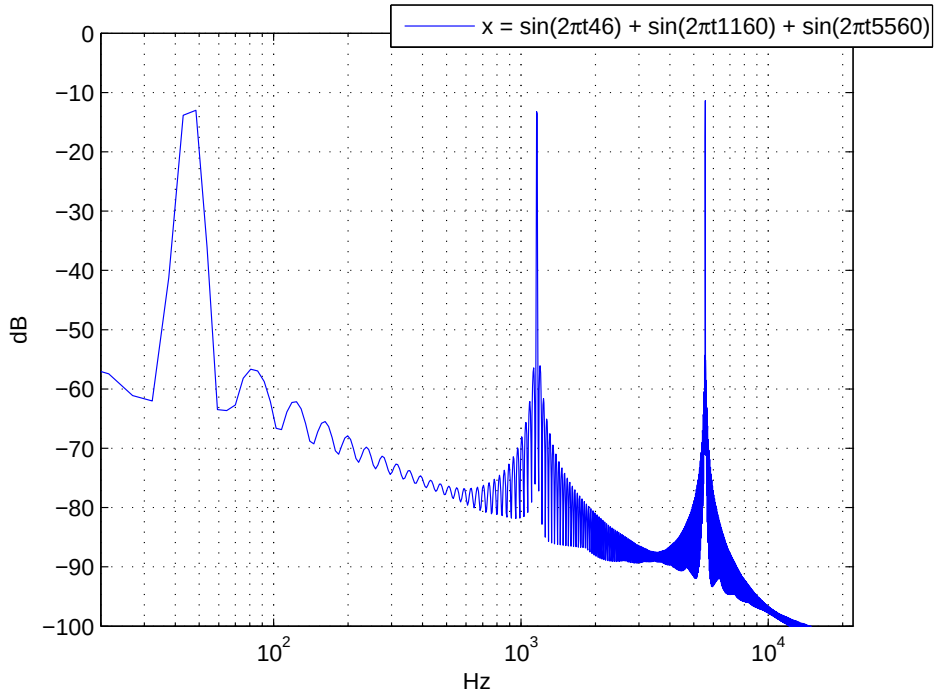

Figure 5: Frequency domain representation of the sinusoidal disturbing signal.

It is clear that the secondary path with the highest accuracy is not necessary. Nevertheless, a certain accuracy is still needed in order to avoid the big oscillations seen for smaller step sizes. The algorithm's performance will decrease once the length of $\hat{S}$ is extremely reduced, see the referenced error signals for a secondary path's length of 256 taps and shorter. Still, the algorithm remains stable for the cases considered. Apparently it is not necessary to implement the secondary path's estimation with great accuracy, at least not for the $Feedforward$ structure and when cancelling a periodic disturbing signal. The error signal fades away even for great disparities between the secondary path S and its estimation $\hat{S}$.

Another way of simulationg an inequality between the secondary path and its estimation, is simply by choosing $S \neq \hat{S}$. Illustrated in Fig. 7 are the referenced error signals for the extreme cases taken into consideration from Fig. 4, i.e. $TF_{leak-proof}$, TF_{1sl} and TF_{2sl}. These are the measured secondary paths when the headphones were positioned in a leak-proof manner on the dummy head and two other for which air leakages were simulated by introducing, between the dummy head and the headphones, one and two conic slots, respectively. The secondary path's estimation is assumed to be $\hat{S} = TF_{leak-proof}$ while the step size is kept as before at $\mu = 0.001$. The length of S is set at 4096 taps and a reduced one of 128 taps is chosen for its estimation $\hat{S}$.

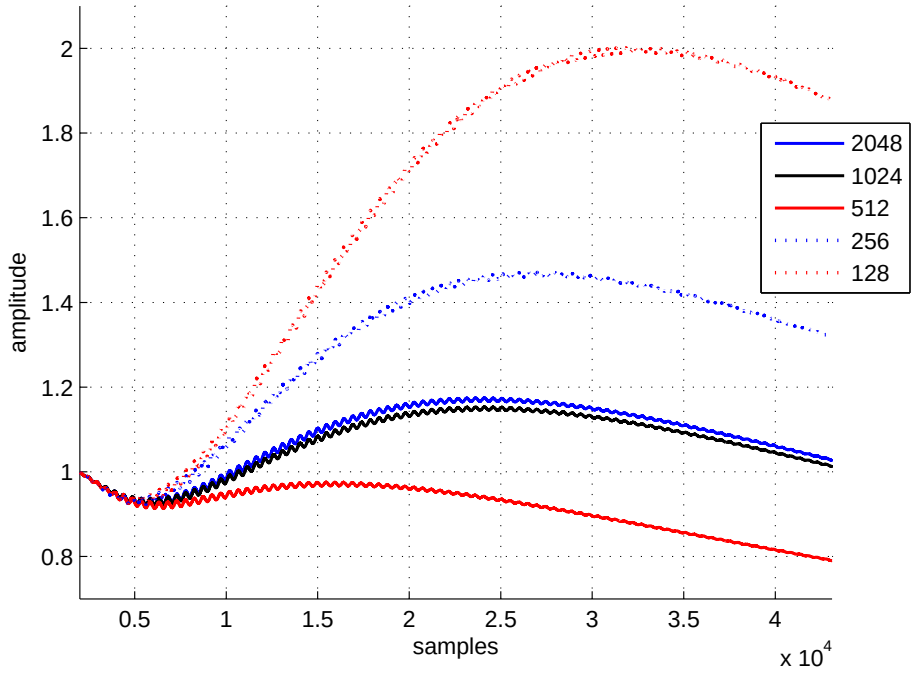

Figure 6: Referenced squared error signal for different lengths of the estimated secondary path.

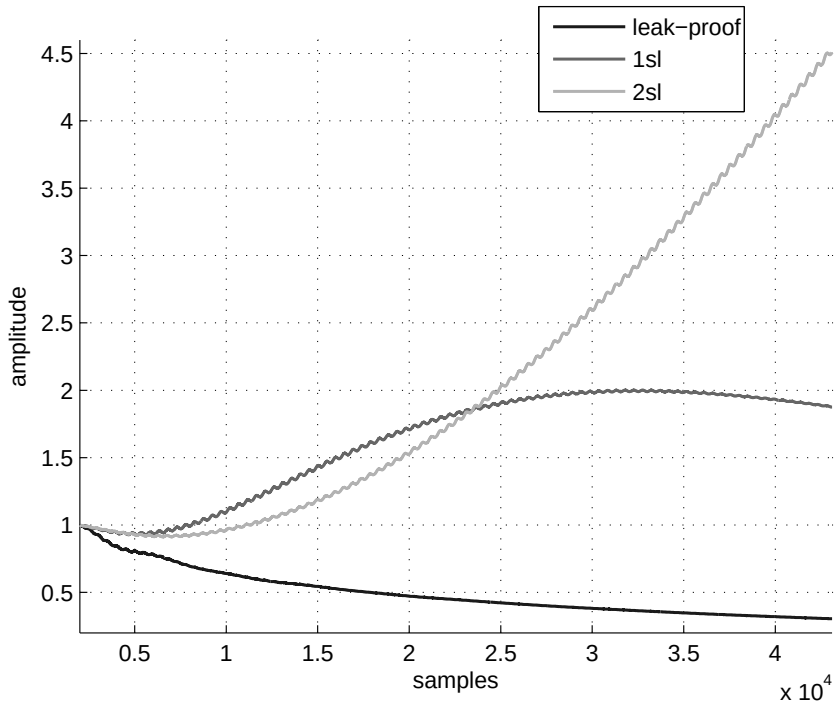

Figure 7: Referenced squared error signal for different secondary paths S.

The case for which $S = TF_{2sl}$ becomes unstable and will not longer be considered since it does not represent a realistic scenario. The other two cases on the other hand, define the spectrum between wearing the headphones in a leak-proof and in a leaky [11] manner. This is why mainly these two transfer functions are considered for the subsequent analysis.

By analysing the referenced error signals of both extreme cases, i.e. black and dark grey curves in Fig. 7, it becomes clear that identifying the secondary path will not improve significantly the algorithm's performance. The disturbing signal is cancelled for both cases. Whether or not Eq. 3 is valid does not seem to be relevant with these settings although a slight better performance is still evident if approximating the latter equation.

Other simulations with the $Feedforward$ structure, see Fig. 1, were done both in $Matlab$ and $PureData$. All of them point to the same conclusion, it is not relevant to identify the secondary path nor to implement its estimation with high accuracy. The algorithm works fine and stays stable even if wearing the headphones in a leaky manner.

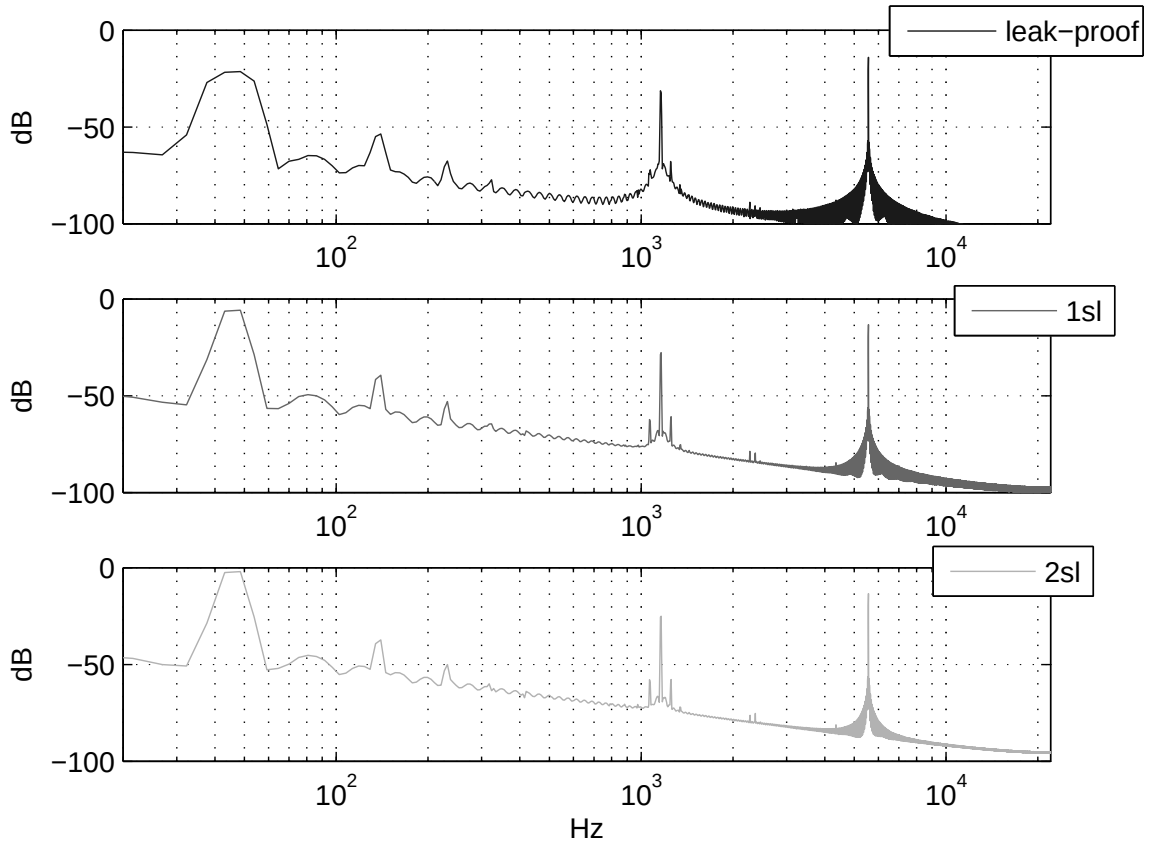

Figure 8: Frequency domain representation of the curves in Fig. 7.

11. One air leakage is found at the most.

Fig. 6 and Fig. 7 give a good overview on the algorithm's performance and stability. Beyond that it would be useful to analyse the error signal in the frequency domain to see the frequency ranges where the algorithm works better. This is done by generating a $Welch - Periodogram$ of the signal under study. Essentialy it is a calculation of the signal's power spectral density in blocks. The goal is to illustrate the signal's energy at defined frequency bins. A total of eight blocks are decomposed with a 50% overlapping between them. Each block is then filtered with a $Hanning$ window and all of them together yield the periodogramm seen in Fig. 8.

A better performance for middle and higher frequencies is evident. Most of the error signal's energy lies in the lower frequency domain and becomes larger the more S and $\hat{S}$ differ from each other. This can be explained by observing Fig. 4, where the largest differences between the secondary paths are found at lower frequencies precisely. The algorithm is more sensitive at lower frequencies, especially when S and $\hat{S}$ drift away from each other. When comparing the residual noise from Fig. 8 to the disturbing signal illsutrated in Fig. 5, it becomes evident that noise is actually being generated at lower frequencies as a result of the noise cancelling process once Eq. 3 is not valid. The disturbing signal itself had an amplitude of about $-10dB$.

3.1.2 Feedback Structure

The next simulations were done as before with the unique difference of the algorithm's structure. The length of the estimated secondary path was, as in Fig. 6, reduced while keeping the step size at a constant value of $\mu = 0.001$. The worst case scenario is given by implementing both extreme cases defined before. Once again, it is wrongly assumed that the listener wears the headphones in a leak-proof manner, i.e. $\hat{S} = TF_{leaf-proof}$ and $S = TF_{1sl}$. Being able to identify the secondary path will not be of interest if stability is given and the disturbing signal is cancelled.

As for the $Feedforward$ structure, there are no significant improvements when increasing the length of $\hat{S}$. As seen in see Fig. 9, the referenced error signal is cancelled for both cases. Both curves are alike and no benefit comes from a more accurate implementation of $\hat{S}$. The plots in Fig. 9 are both the same. The upper one shows the referenced error signals for a simulation time of one second while the lower one is a closer display of the first 150 samples.

Implementing a completely different secondary path estimation $\hat{S}$ has a bigger influence on the algorithm's performance than reducing its length. To accurately identify and implement the secondary path appears not to be that relevant, at least for large latencies and when cancelling sinusoidal disturbing signals. The latter is cancelled, as shown in Fig. 10, for the two extreme cases in a similar manner.

The determining factor for the algorithm's performance are still the latency of the system and the step size chosen. Both will be discussed in detail later in this section.

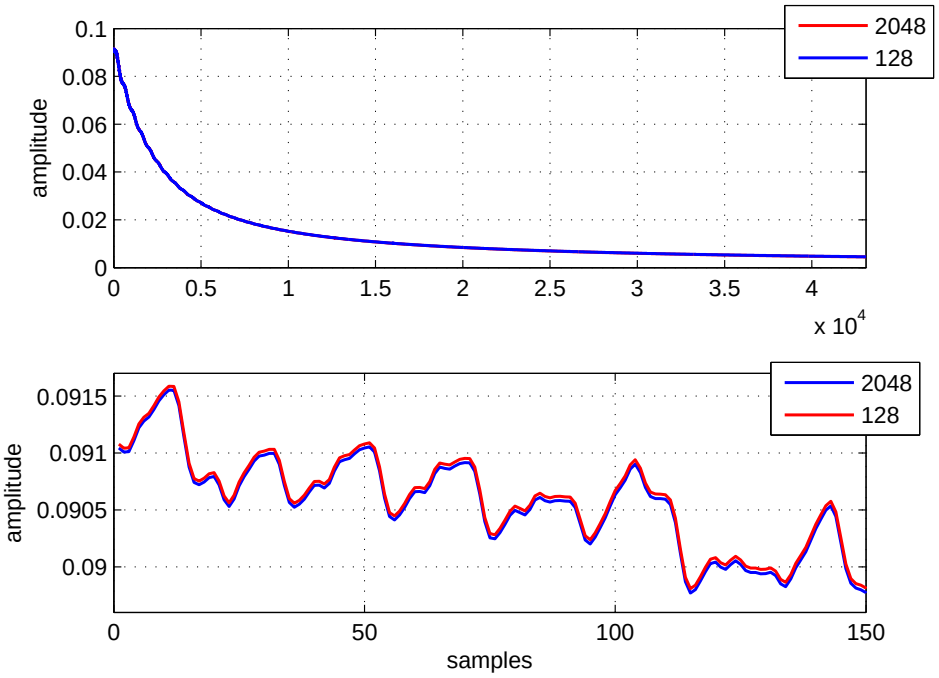

Figure 9: Referenced squared error signals when estimating S with a high and low accuracy.

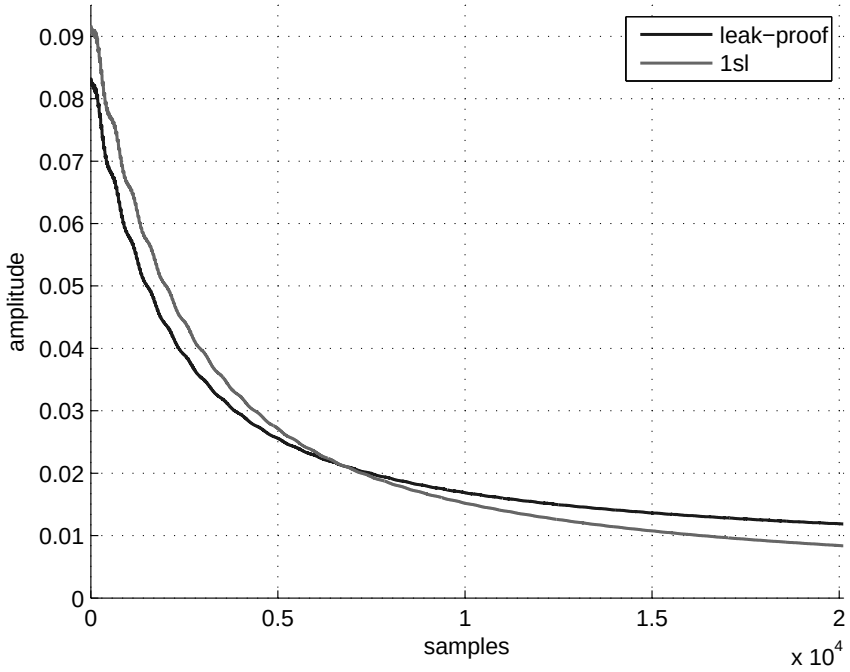

Figure 10: Referenced squared error signals when implementing two of the extreme cases depicted in Fig. 4 for $\hat{S}$.

3.2 Low Latencies

A digital noise cancellation system for headphones with a low latency was realised in the master thesis of Teschinegg, see [Tes12]. This system permits amongst other things to cancell more effectively lower frequencies. With this in mind, a new set of simulations for lower latencies became meaningful and realisable if desired. The next step in the work presented here was to simulate the noise cancelling process for a broadband disturbing signal. Such simulations are definitely much more decisive than the ones made in Section 3.1 since in reality most of the disturbing signals have a broadband and stochastic nature. The simulations were done for both structures discussed so far while staying confined to the two extreme cases defined earlier in this section.

The latency of the system Δt was set at 0.05ms enabling a simulation with white noise as the disturbing signal. This latency represents a delay of two samples for each conversion made. The lengths of the secondary path and its estimation stayed unchanged at 4096 and 128 taps, respectively.

3.2.1 Feedforward Structure

The two extreme cases chosen from Fig. 4 are again the basis of the next simulations. These comprise two possibilities when wearing the headphones, i.e. in what was defined to be a rather leak-proof or a leaky manner. Furthermore, two scenarios are possible depending on the choice when implementing $\hat{S}$.

Depicted in Fig. 11 is the case when assuming that the headphones are worn in a leak-proof manner. The red curve is the referenced error signal when Eq. 3 is valid. The blue curve represents the worst case scenario where $\hat{S} = TF_{1sl}$. A better cancellation of lower frequencies around $30Hz$ - $40Hz$ can be seen. Nevertheless it appears one more time that knowing the secondary path is not as important as it seemed. At least not for this structure and when the headphones are worn in a leak-proof manner.

Illustrated in Fig. 12 are the same curves from Fig. 11 in the frequency domain. This representation just confirms the conclusions made so far.

A worst performance is expected if the headphones would be worn in a leaky manner, here simulated by $S = TF_{1sl}$. The referenced error signals are illsutrated for both scenarios in Fig. 13 while their frequency domain representation is found in Fig. 14. The algorithm appears to work just as good as before, even if the headphones are not worn in an optimal way. A slight better performance is given when implementing an estimation of S with a flatter spectrum, i.e. $\hat{S} \longleftrightarrow TF_{leak-proof}$. For that scenario a better cancellation of up to $3dB$ is achieved at lower frequencies, see Fig. 12 and Fig. 14. It is evident that Eq. 3 does not have to hold for the disturbing signal to be cancelled. Identifying the secondaray path will not improve the algorithm's performance in a significant way and is thus not really necessary for this structure.

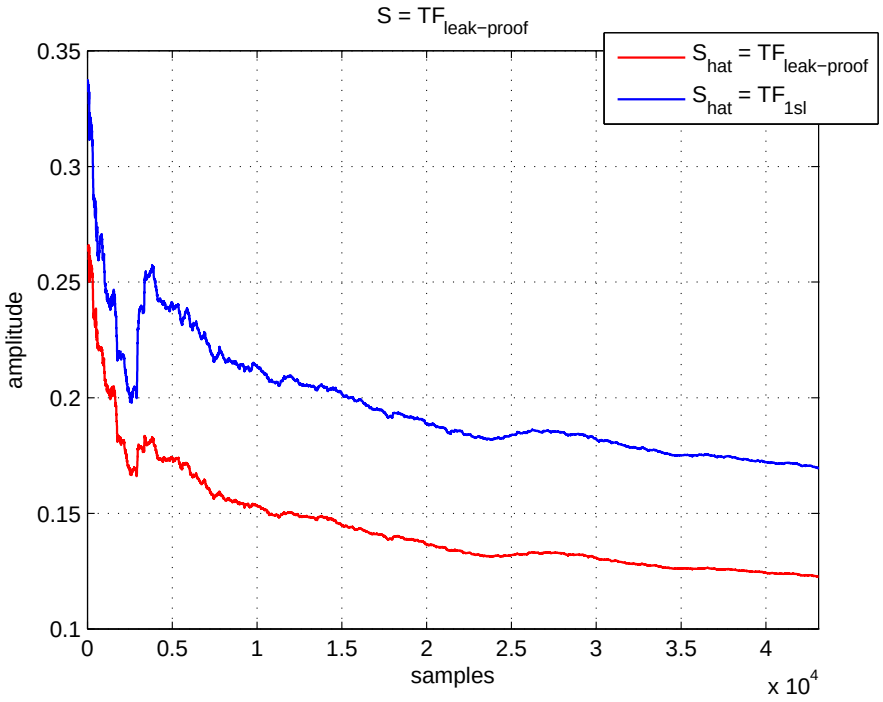

Figure 11: Referenced squared error signals when cancelling a broadband signal once the headphones are worn in a leak-proof manner.

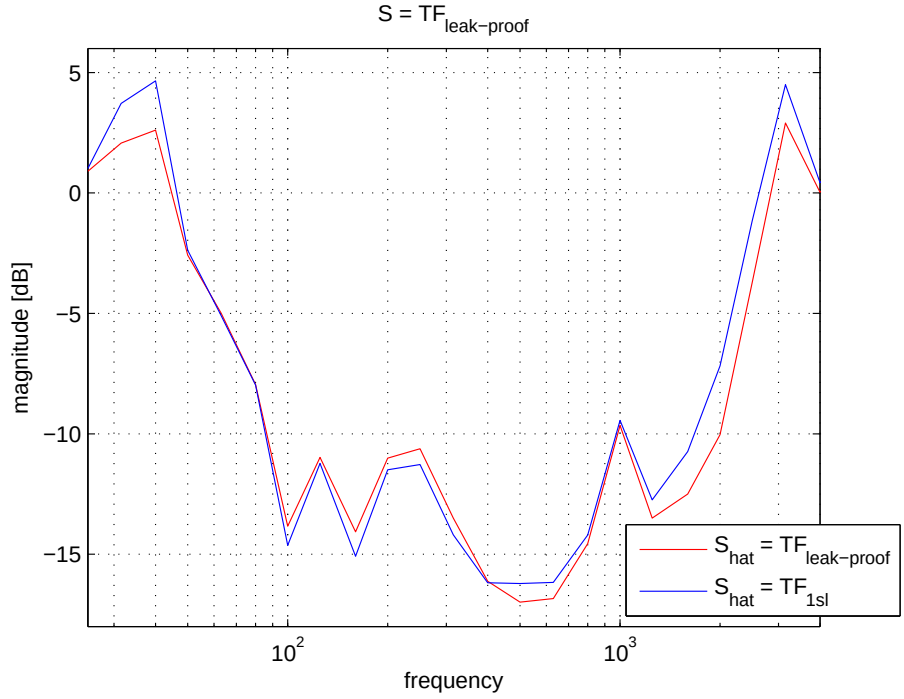

Figure 12: Frequency domain representation of the curves in Fig. 11.

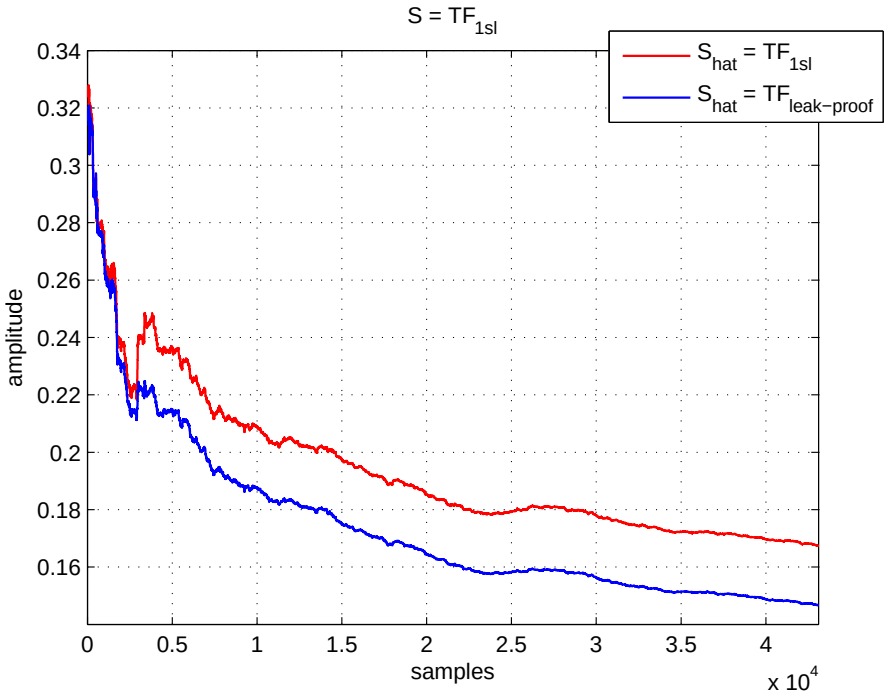

Figure 13: Referenced squared error signals when cancelling a broadband signal once the headphones are worn in a leaky manner.

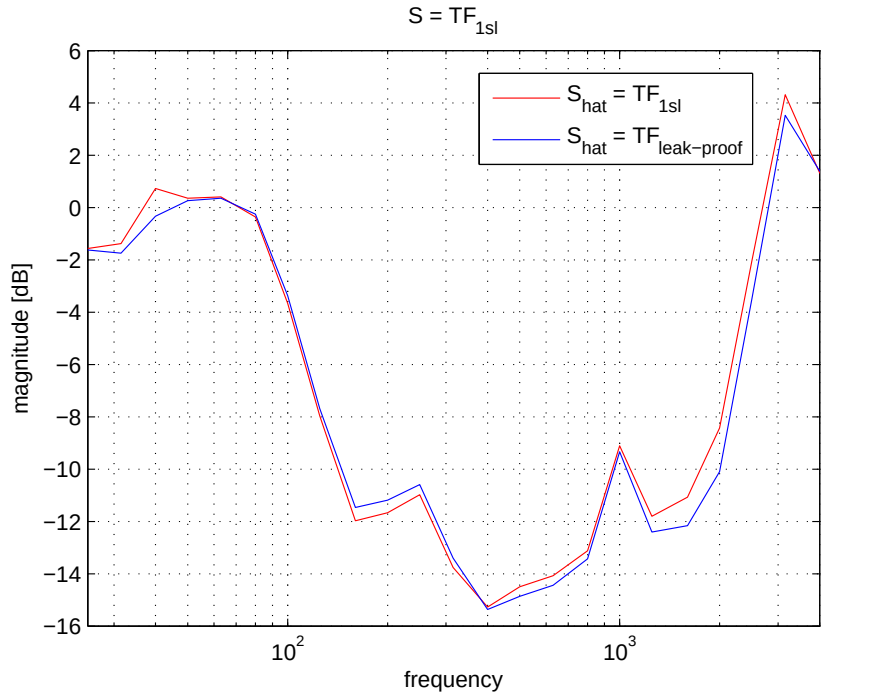

Figure 14: Frequency domain representation of the curves in Fig. 13.

3.2.2 Feedback Structure

The parameters stayed the same as before for the next simulations. These were a latency of $\Delta t = \ 0.05$ ms, a step size $\mu = 0.001$ and white noise as the disturbing signal. The same scenarios are again considered. This time the $Feedback$ structure for the LMS algorithm was studied (see Fig. 2).

For the first case it is once more assumed that the headphones are worn in a leak-proof manner. As seen in Fig. 15, the referenced error signal fades away for both estimations of the secondary path S. The algorithm stays stable and the disturbing signal has already been cancelled after approximately 500ms. There are no important differences when analysing both curves in the frequency domain either, see Fig. 16. However, a slight better performance is visible for lower frequencies once $S = \hat{S}$. Other than that, it seems that accurately implementing and knowing the secondary path is not an important factor when aiming at improving or guaranteeing the noise cancellation process once the headphones are worn in a more or less leak-proof manner.

Next, it is assumed that $S = TF_{1sl}$, which means that the headphones are worn in a leaky manner. Given the implemented structure, a bigger influence of the secondary path's estimation $\hat{S}$ on the algorithm's performance is expected, see Section 2.2.2. Illsutrated in Fig. 17 are the referenced error signals for both extreme cases considered so far. As seen for the blue curve, the algorithm diverges due to the large disparities between S and $\hat{S}$. It is clear that the algorithm becomes unstable once $S \neq \hat{S}$.

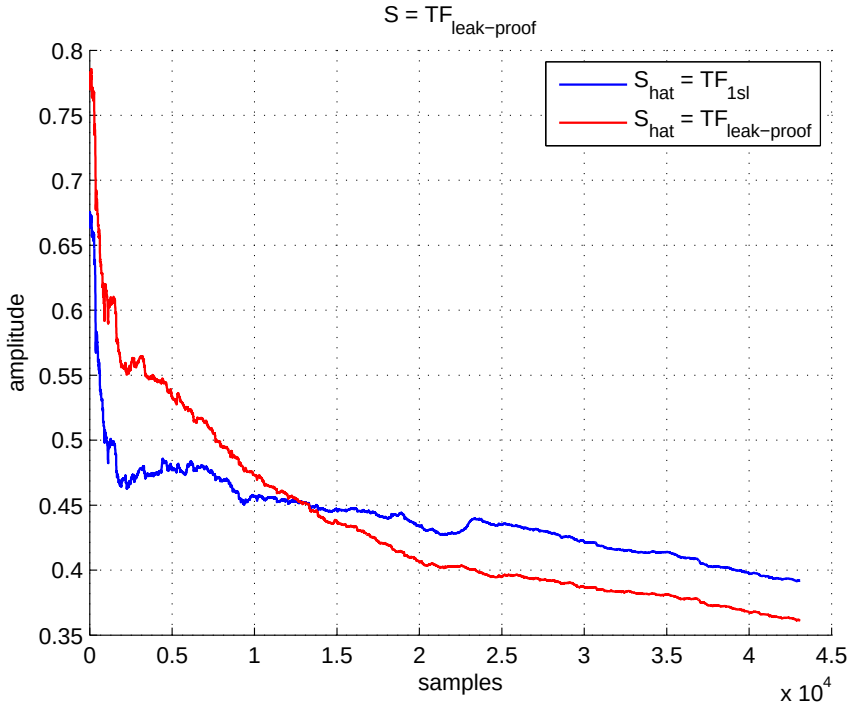

Figure 15: Referenced squared error signals when cancelling a broadband signal once the headphones are worn in a leak-proof manner.

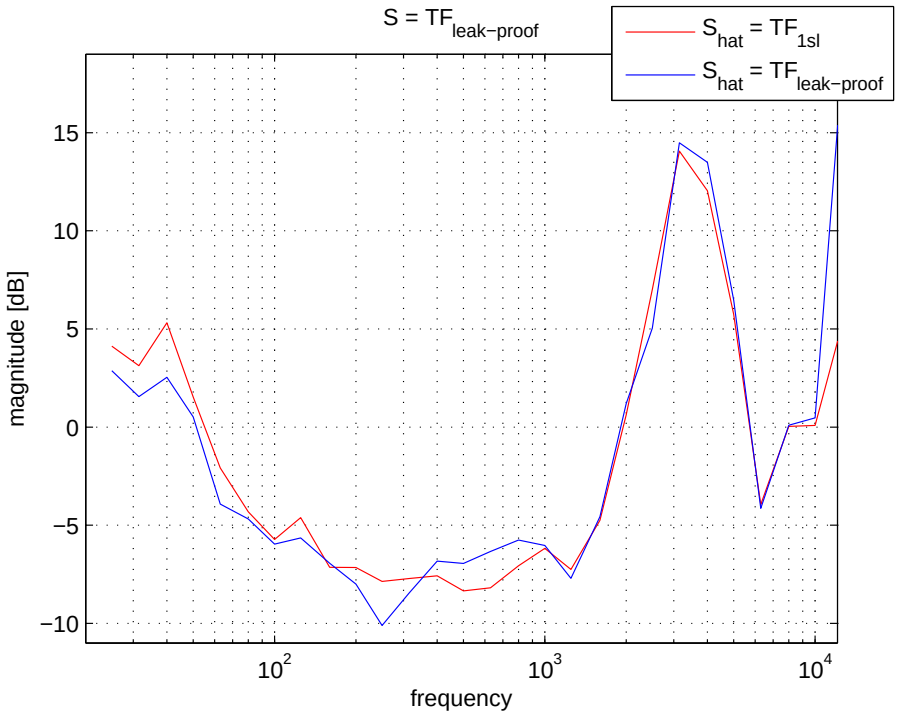

Figure 16: Frequency domain representation of the curves in Fig. 15.

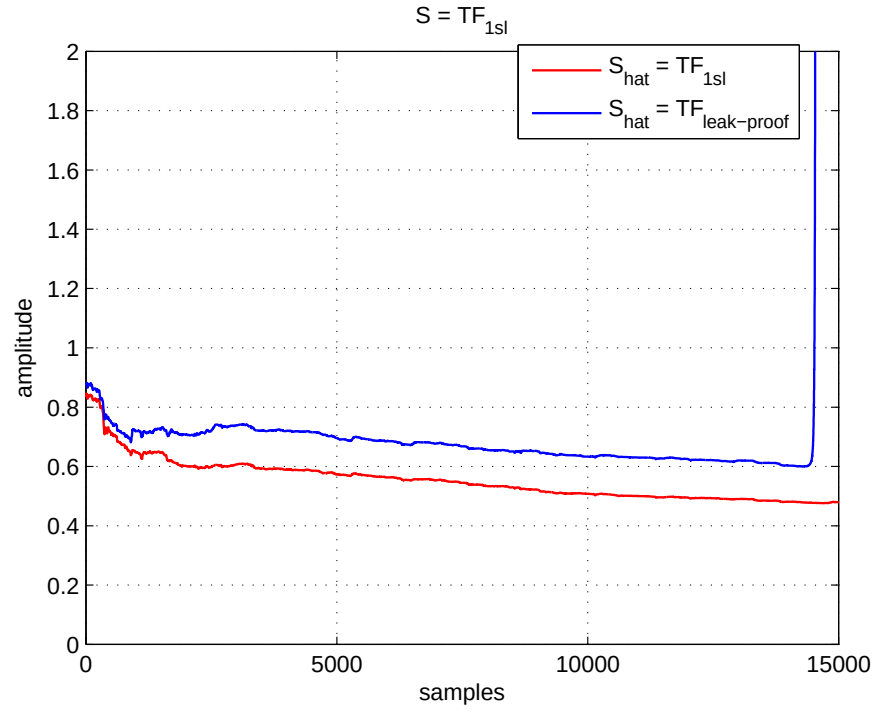

Figure 17: Referenced squared error signals when cancelling a broadband signal once the headphones are worn in a leaky manner.

The secondary path's estimation has also a major influence on the algorithm's stability for the $Feedback$ structure. It is important to remember that $\hat{S}$ is used a second time for this structure. The effects of S cannot be fully removed by $\hat{S}$ if large disparities between them are given. The red curve shows that the disturbing signal can still be cancelled if Eq.3 holds. On the other hand, the algorithm becomes unstable once $S \neq \hat{S}$. A frequency representation of the curves in Fig. 17 would not provide further information since stability is not given.

As seen in Fig. 17, identifying the secondary path is necessary in order to guarantee the algorithm's stability. A more appropriate transfer function for implementing $\hat{S}$ could be chosen out of a data base given the secondary path is known. The disturbing signal can still be cancelled by reducing the disparities between S and $\hat{S}$ or at least approximating Eq. 3. The accuracy needed for this approximation will be discussed later in Section 5. For now, it has been shown that an identification of the secondary path is needed for the $Feedback$ structure. Especially when the headphones are not worn in a leak-proof manner.

3.3 Step Size

A good choice of the step size, also called learning rate, will ensure a fast and efficient convergence of the algorithm. Is it too small, then the $Wiener$ solution [12] can still be found but way to slowly for the intended performances. Is it on the other hand too large, then the algorithm cannot converge to the minimum of the cost function [13] and thus the algorithm becomes unstable. Many approaches [LP02], [SH94] et al. have been proposed in order to compute the largest possible value of the step size μ for which stability is still given.

One major conclusion has been made in these studies, the bigger the latency of the system, the smaller is going to be the maximal step size μ_{max} and thus the slower will the algorithm converge. In other words, the maximal value for μ, for which stability is still given, is inversely proportional to the system's latency. The method used in this section was first introduced by $Snyder$ and $Hansen$ in [SH90]. Furthermore, simulations for a low latency, i.e. $\Delta t = 0.05$ms, and with broadband noise as the disturbing signal are presented and compared to the theoretical values obtained using Eq. 9.

Scott Snyder and Colin Hansen propose a stability criterion in [SH94] for the step size of the FxLMS algorithm. This one states that the maximal value for the step size μ_{max} is inversely proportional to the maximal eigenvalue λ_{max} of the autocorrelation matrix $\mathbf{R}_{xx}$. The ralationship is given by Eq. 9 where d_n is the acoustic time delay expressed in sample periods and is defined as $d_n = \tau \cdot f_s$. The sampling frequency f_s is set by default

12. The derivation of the $Wiener$ solution can be found in [Hay02].
13. It is defined as the 1^{st} moment of the squared error, $\zeta = E\{e^2[n]\}$. For more information concerning the costfunction please refer to [Hay02].

at $44.1kHz$ and τ is the system's latency expressed in seconds.

$$0 < \mu < \left(\frac{1}{\lambda_{max}}\right) \cdot sin\left(\frac{\pi}{2 \cdot (2d_n + 1)}\right) \tag{9}$$

This can be understood by the nature of the algorithm. Basically it moves the adaptive filter coefficients $\mathbf{w}[n+1]$ in direction of the negative gradient, see also Section 2.1. If the eigenvalues of $\mathbf{R}_{xx}$ are large, then the gradient of the costfunction is going to be large too. By additionally chosing a large value for μ it becomes imposible to reach that minimum and the algorithm diverges. Eq. 10 gives the gradient of the cost function where $x[n]$ is the disturbing signal, $y[n]$ is the anti-noise signal, $\mathbf{R}_{xx}$ is the autocorrelation matrix and $\mathbf{w}[n]$ is the adaptive filter coefficient vector.

$$\nabla\zeta = -2E\Big\{x[n] \cdot \mathbf{y}[n]\Big\} + \Big\{\mathbf{R}_{xx} \cdot \mathbf{w}[n]\Big\} \tag{10}$$

The autocorrelation matrix $\mathbf{R}_{xx}$ can be cumputed by using Eq. 11. Once this matrix is available, its maximal eigenvalue can be identified and used in Eq. 9 in order to find the theoretical maximal value for the step size. The filtered reference signal $\mathbf{x}_f[n]$ is obtained by convolution of $x[n]$ and the secondary path S.

$$\mathbf{R}_{xx} = E\Big\{\mathbf{x}_f[n] \cdot \mathbf{x}_f^T[n]\Big\} \tag{11}$$

Next, it is assumed that Eq. 3 is valid while the secondary path S is described by the transfer function $TF_{leak-proof}$ from Fig. 4. The maximal value for μ using Eq. 9 yields $\mu_{max} = 0.18595$. With this value in mind a new set of simulations was done for both structures. The results are presented in Fig. 18.

The step size was increased progressively for both structures in order to see the direct influence of the step size on the referenced error signal. It is evident that no better performance of the algorithm is achieved by increasing the value of μ. The smallest value used for this simulations where $\mu = 0.01$ is already a good trade-off for these settings. The theoretical maximal value is concordant with respect to the simulations made in Fig. 18, especially for the $Feedback$ structure where the algorithm becomes unstable for a step size of 0.01.

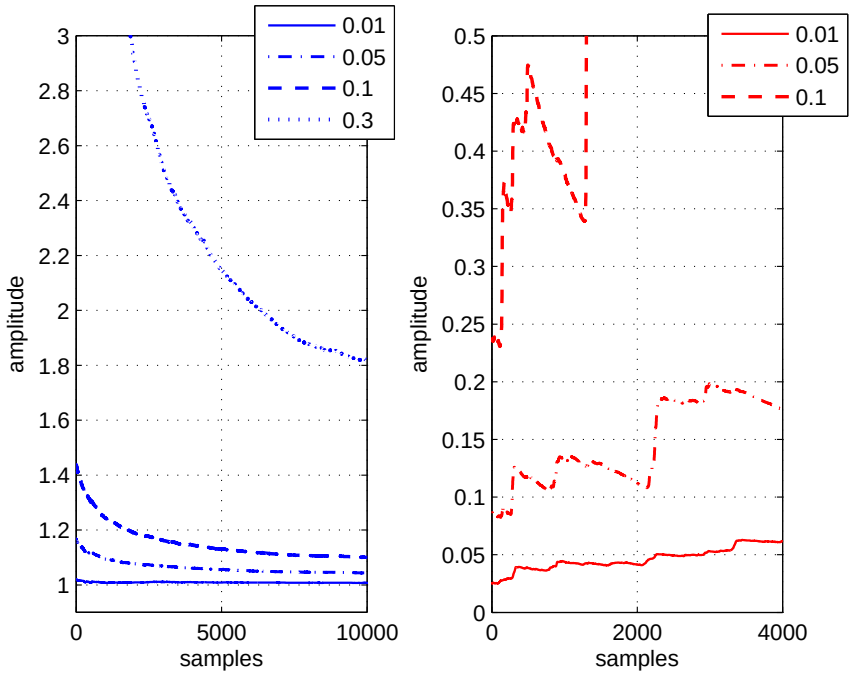

Figure 18: Referenced squared error signals with different values for the step size. To the left the $Feedforward$ and to the right the $Feedback$ structure.

3.4 Corollary

With the results obtained in this section it becomes possible to say that for the $Feedforward$ structure it is not relevant to accurately know nor estimate the secondary path S. The algorithm works better once the headphones are worn to a degree in a leak-proof manner. Nonetheless, it will also work fine if the headphones are worn in a leaky manner. Being able to identify the secondary path is also not necessary and hence not interesting for this structure.

For the $Feedback$ structure on the other hand, it is very well important to identify whether the headphones are being worn in a rather leak-proof or leaky manner. The algorithm's stability and thus an effective cancellation of the disturbing signal depends on it (see Section 3.2.2).

The maximal value for the step size and the effectiveness of the algorithm is inversely proportional to the system's latency. Having fast AD and DA converters is desired in order to improve the algorithm's performance. An overall better performance can be achieved by choosing an optimal value for the step size and by identifying the secondary path. The latter enables a more addecuate choice of a transfer function in order to remove the effects introduced by S. Especially for the the $Feedback$ structure where, as shown in Fig. 2, $\hat{S}$ is needed an additional second time.

4 Measurement

4.1 Measurement Construction

The measurements took place at the IEM in Graz in a rather small room [14] next to the offices in the 1^{st} floor. The walls as well as the ceiling are covered with absorbers in order to minimise reflections. The room can be seen in Fig. 19. Also the side wall, where the entrance is to be found, is separated by a thick curtain from the working environments next to it. The room dimensions with these measures result in a reverberation time RT_{60} of approximately $50\ ms$. [15]

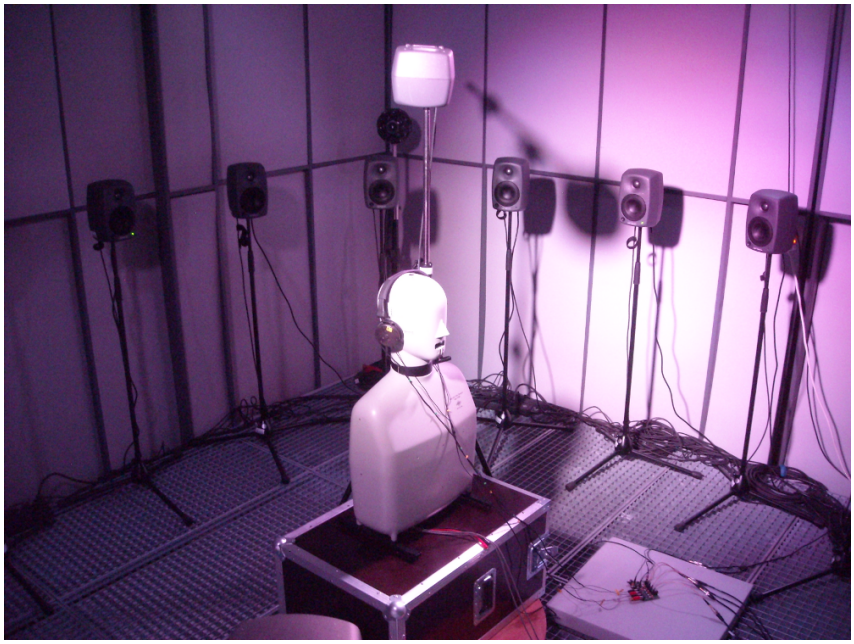

Figure 19: Measurement setup at the IEM's 1^{st} floor, GRAZ, AT.

A total of five $Genelec\ 8020$ loudspeakers [16] were used for the measurement of the secondary paths. As seen in Fig. 20, four of them were spaced on a circle with a radious of about $1,68$ m in $90°$ steps. A hight of $1,20$m was chosen for the loudspeaker's epicentre [17]. This choice can be explained by the fact that the listener's ears (when sitting) are found on average at that hight precisely. A fifth loudspeaker was positioned 50cm above the dummy head. Furthermore, headphones with ANC were used on the dummy head resulting in a total of seven reproducing points. The microphones are found two for each side of the headphones and other two built in the dummy head, one for the right and another for the left channel, respectively.

14. The room dimensions are (3.7mx3.7mx3.2m).
15. For the precise definition of the RT_{60} and other definitions for the reverberation time please refer to [Goe06].
16. There are more loudspeakers visible in Fig. 19 than they were actually needed for the measurements. The actual loudspeaker configuration is illsutrated in Fig. 20.
17. The centre of the loudspeaker's membrane was defined as the epicentre.

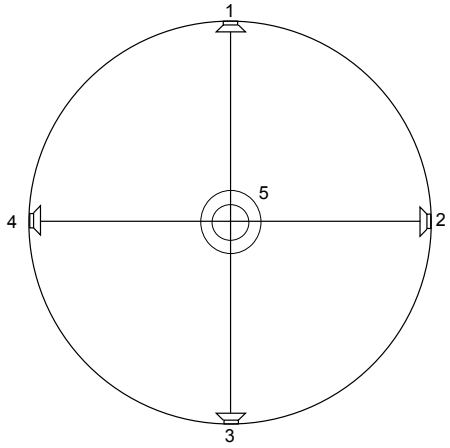

Figure 20: Loudspeaker array used for the measurements.

4.2 Measurement Signal

The signal used for the impulse response measurement discussed above was fabricated in $Matlab$. Given the situation, an exponential sweep signal [18] was chosen because it is a rather fast and very robust method.

The measurement signal has a frequency range going from 10Hz to 10kHz. The time needed to cover this range, i.e. the $sweep-time$, was set to one second while keeping the sampling frequency at 44,1kHz. The exponential sweep is depicted in Fig. 21 in its frequency domain representation. In order to ensure a good signal-to-noise ratio [19], a gain of 85dB(A) was applied to the signal while keeping the ambient noise as low as possible during measurements.

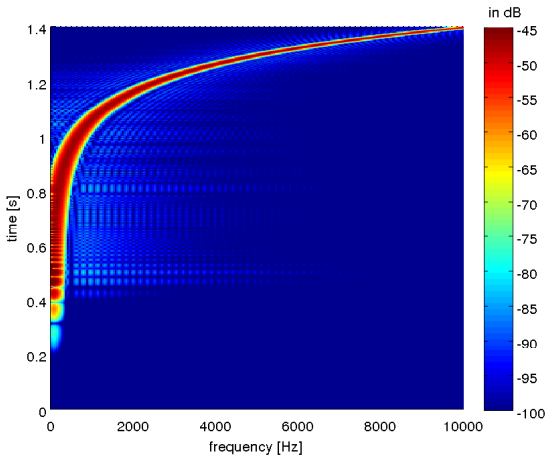

Figure 21: Exponential sweep in the frequency domain.

18. Signal in which the frequency of the signal varies with a geometric relationship over time. In this case, it varies exponentially as a function of time.

19. Logarithmic measure that compares the level of a desired signal to the level of background noise. It is defined as the ratio of the signal power to the noise power.

4.3 Measured Secondary Paths

These measurements were done before knowing the results of the simulations presented in Section 3. Originally, a secondary path identification for both structures, i.e. $Feedforward$ and $Feedback$, was planned. Measurements with the outside microphones of the ANC headphones were done for the first one. They will not be presented anymore since the focus of the work is henceforth to identify the secondary path for the $Feedback$ structure. For this structure only two inner microphones are needed (see Fig.2). Also, the measurements done using the loudspeaker array depicted in Fig. 20 are not necessary anymore. Again, these were thought for the $Feedforward$ structure, where the incidence angle of sound is of extreme importance, especially for the external microphones.

The measurements of interest were realised by reproducing the measurement signal, see Fig. 21, with the ANC headphones and by recording it with the inner microphones of the ANC cancelling system. Four measurements were done on the dummy head using some of the methods already seen in Section 3 for simulating air leakages. These correspond to the black curves illustrated in Fig. 22 and in this particaular order, $2sl$, $1sl$, $leak-proof$ and $leak-proof\ and\ tied$. The other eight curves were obtained by measuring four test subjetcs two times each. For the first measurement they were asked to wear the headphones in a leak-proof manner. For the second one they were asked to shift the headphones and wear them in a leaky manner.

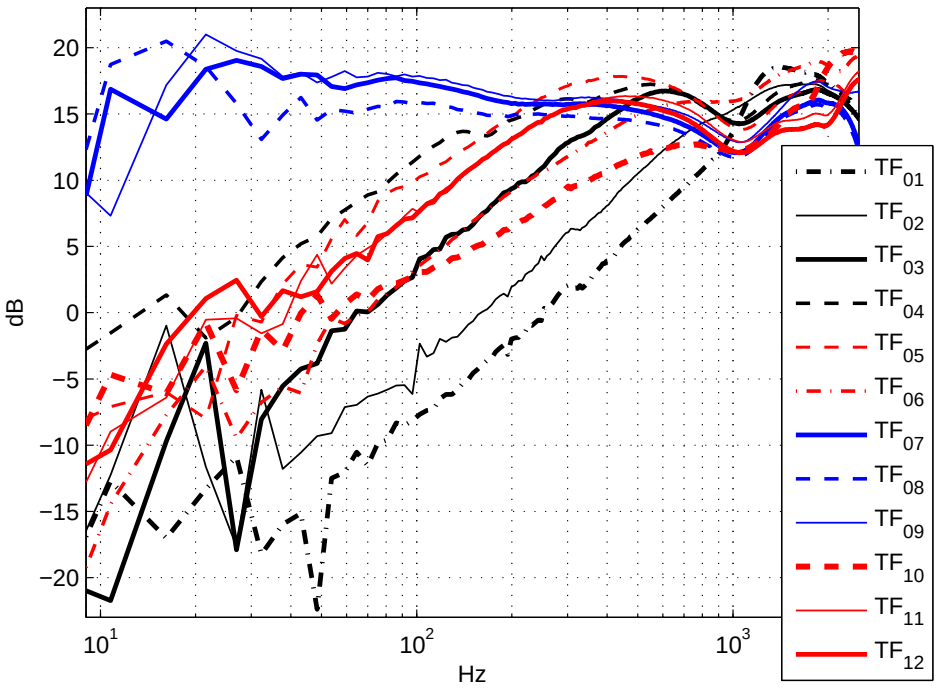

Figure 22: Magnitude response of the measured secondary paths for the left channel.

The goal here was to make a set of measured secondary paths available. Whether or not the test subjects were able to actually shift the headphones from a leak-proof into a leaky manner of wearing them is not really relevant. After all, they wore them in what they thought was a leak-proof and a leaky manner, respectively. The result from a total of twelve measurements is depicted in Fig. 22.[20] These are the secondary paths obtained for the left channel. The measurements for the right channel look alike but with a slight lower amplitude level which is why the left channel was favoured. The reason for lower amplitudes is presumably the potentiometer itself. This factor influences the absolute value of the measurements only and leaves the characteristics of the obtained curves unchanged.

A normalisation of the secondary paths was still necessary in order to arrive to these results. A reference measurement, where the measurement signal was sent directly from the DA- to the AD-converters, was made in order to consider the system's latency as well. The transfer functions were cut off in their time domain representation by the adequate time, i.e. the sytem's latency, and thus substracting the unwanted digital path of the system.

20. The choice of the reamining colours for plotting the secondary paths is discussed in Section 5.

5 Secondary Path Identification

5.1 Identification Method

As already proposed in Section 2.4, the idea for identifying the secondary path is to leak a $15Hz$ sinusoidal signal when the headphones are being worn. The new $Feedback$ structure with the additional test signal $t_s[n]$ is illustrated in Fig. 23. The test signal is added to the anti-noise signal generated by the adaptive filter and is reproduced by the loudspeakers as well.

It is evident that a compensation of the test signal is necessary for the algorithm to work properly. This is done by subtracting the filtered and delayed test signal from the residual noise signal $e_{in-ts}[n]$. The first one is delayed accordingly in order for it to be aligned in time with the residual noise signal and is also filtered with $\hat{S}$ for compensating the effects introduced by S. By means of subtraction of both signals it is possible to generate the correct residual noise signal $e_{in}[n]$ that is needed for the LMS algorithm.

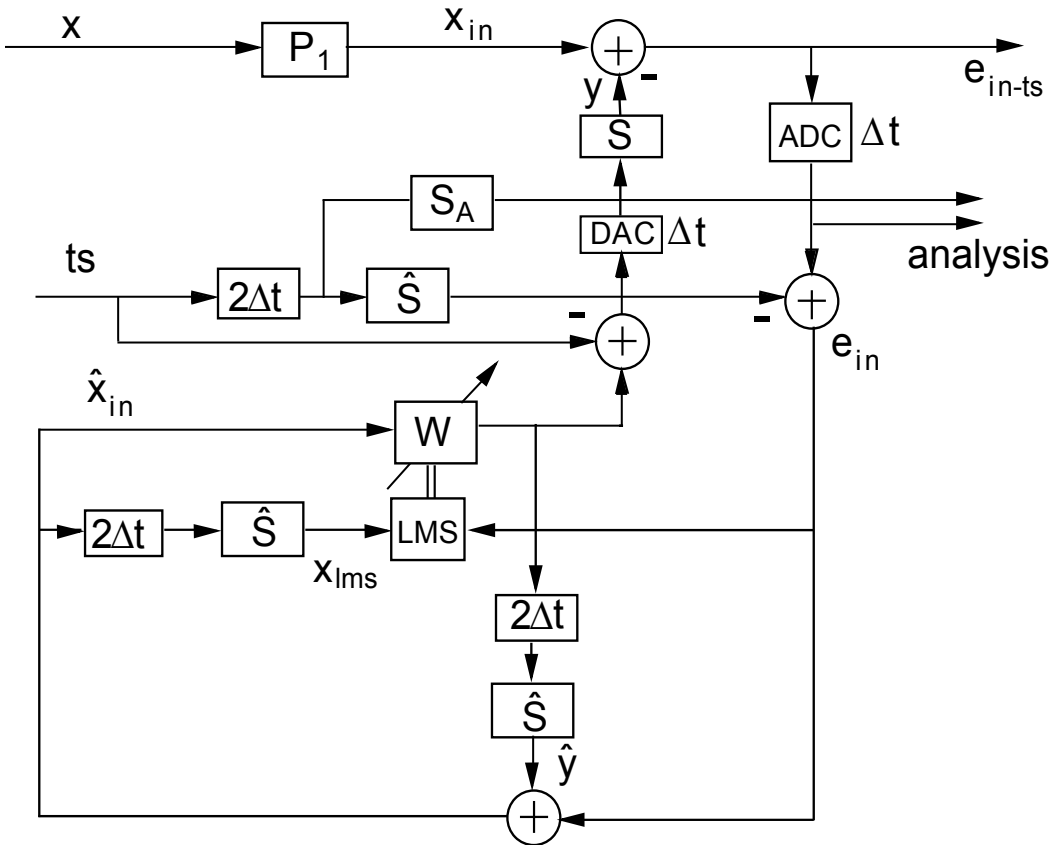

Figure 23: Feedback structure with an additional test signal.

The additional secondary path denoted as S_A is used in order to obtain the statistical relationship between the test and residual noise signals. A transfer function from the first set of curves is taken for the implementation of it in order to obtain a high cross-correlation in case the headphones are being worn in a leak-proof manner. With this choice a low cross-correlation will arise if there is an air leakage found, facilitating the decision for implementing $\hat{S}$. More about the statistical relationship between $e_{in}[n]$ and $t_s[n]$ in Section 5.3.

The test signal was placed at $15Hz$ and with a gain of $+6dB$ with respect to the disturbing signal. A lower gain level for the test signal would most probably remain undetected by the inner microphone making an identification impossible. Chosing on the other hand a higher gain level is unrealistic since most headphones will not be capable of reproducing those frequencies any more louder. Even if that was the case, loud signals in that frequency range are not considered to be sane for the human ear.

The outcome of the noise cancelling process is delivered by the inner microphone and is depicted exemplarily in Fig. 24 using white noise as the disturbing signal and for a secondary path belonging to the first set of curves. Implementing a transfer function of this group means that the headphones are being worn in a leak-proof manner and that the test signal can be measured by the inner micophones. That is exactly what can be seen at the test frequency, where both curves differ in their magnitude levels for about $6dB$ precisely. The black curve in Fig. 24 constitutes the residual error signal $e_{in-ts}[n]$ with the test signal while the curve plotted in gray is the disturbing signal $x[n]$.

Adding the test signal does not influence the cancelling process in any way with the exception of the magnitude level at the test frequency. This simulation can be seen in Fig. 24 where the cancellation of the disturbing signal in the relevant frequency range is evident while the inaudible test signal remains unmodified.

Cross-Correlation. The cross-correlation is a measure of similarity between two signals as a funciton of time-lag applied to one of them. Its computation is similar in nature to the convolution of two functions. Illustrated in Fig. 25 are the measured secondary paths from Section 4.3 and the correlation gain between them and the sinusoidal test signal $t_s[n]$. The gain level at $15Hz$ is known for both signals, enabling the computation of the correlation values via Eq. 12 and with the goal of determining their statistical relationship.

$$(f \star g)[n] = \sum_{m=-\infty}^{\infty} f^*[m]g[n+m] \tag{12}$$

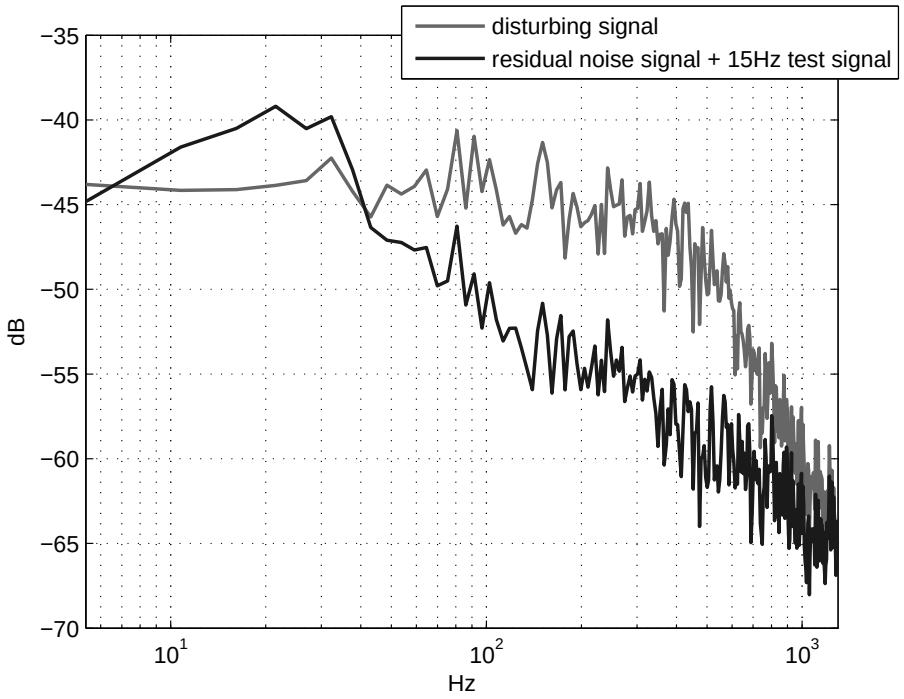

Figure 24: Frequency domain representation of the disturbing signal and its residual error signal with an added $15Hz$ sinusoidal component.

Two tendencies are evident, some of them have a relatively large correlation, i.e. the blue curves, while the majority of them feature a rather small one. It is known that there is no statistical relationship between two signals if they hold a low correlation. If that is the case, then the test signal cannot be fully measured by the inner microphones and therefore an air leakage must be found. The direct consequence is a lower amplitude level of the residual noise signal $e_{in-ts}[n]$ at $15Hz$. Thus the headphones are worn in a leaky manner. For a large correlation it must then follow that the test signal can be measured by the inner microphones, meaning that the headphones are worn in a leak-proof manner. This is the foundation for defining the set of curves in Section 5.2.

5.2 Set of Secondary Paths

The next step is to define sets of curves that can be used for a data base of measured secondary paths. Two sets of curves can be identified from the magnitude response of the measured secondary paths depicted in Fig. 25, i.e. the blue curves separately and the rest of them. The blue curves differ at first sight in the lower frequency range from the others. They also have a considerably higher amplitude level at the test frequency. The main difference however, lies in the correlation values obtained by using Eq. 12. These three blue curves feature a relatively high correlation value that indicates a greater similarity with respect to the test signal than the rest of them. They constitute the first set

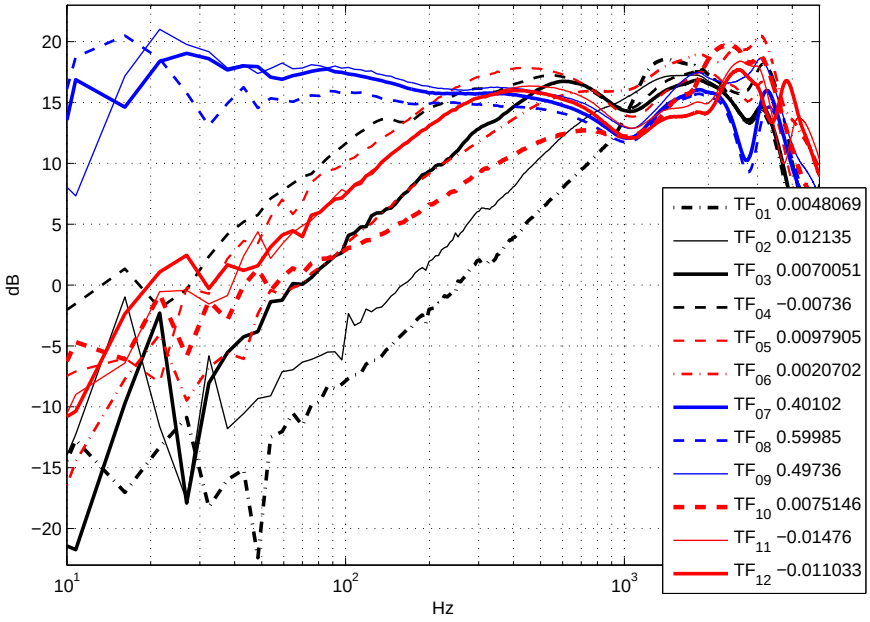

Figure 25: Magnitude response of the measured secondary paths from Section 4.3 with their correlation gain indicated in the legend.

of curves for which the headphones were worn in a leak-proof manner during measurements. The amplitude level for low frequencies will fall considerably once an air leakage is found. This characteristic can bee seen for the black and red curves which form a second set of curves for which a considerably smaller correlation gain is given, thus the leaky group.

The first two black curves correspond to the measurements done on the dummy head where metal tubes were used in an attempt to simulate air leakages. Both cases will not be considered anymore since such an air leakage does not represent a real scenario. The remaining secondary paths are used to characterise the two sets of curves.

Now that two sets of curves have been defined, their stability criteria can be studied. The next simulations are done in the same manner as in Section 3.2.2. The results obtained for the $Feedback$ structure indicated that the algorithm becomes unstable once the headphones are worn in a leaky manner and a secondary path's estimation $\hat{S}$ corresponding to the first set of curves, i.e. the curves for which the headphones are worn in a leak-proof manner, is implemented.

The goal is to find a prototype that describes the second group of curves in Fig. 25, thus the curves with a low correlation gain, for the implementation of the secondary path's estimation. Contrary to the results seen in Fig. 17, the algorithm should remain stable resulting in a cancellation of the disturbing signal. By identifying the secondary path it

becomes possible to chose the adequate secondary path from the data base for implementing $\hat{S}$ and hence guaranteeing the stability of the LMS algorithm. The simulations were carried out with three of the measured secondary paths shown in Fig. 25. These cover pretty much the whole spectrum of the second set of curves [21].

Illustrated in Fig. 26 are five different scenarios. The results go in the same line as the ones obtained in Section 3.2.2. It is clear once again that the algorithm's performance improves once Eq. 3 holds. By implementing a tranfer function from the second set of curves, e.g. TF_{12} for the secondary path's estimation $\hat{S}$, it becomes possible to keep the algorithm stable even if the headphones are worn in a leaky manner and $S \neq \hat{S}$. This case is illustrated by the blue curves in Fig. 26 and constitute a possible solution to the stability problems seen in Section 3.2. These two curves where chosen beacuse they delimit in some degree the range of the second set of curves.

The reamaining three curves depicted in Fig. 26, represent the ideal case where Eq. 3 holds. The algorithm works clearly better for this scenario and even better the less air leakage is present when wearing the headphones. The implemented secondary paths can be found in Fig. 25.

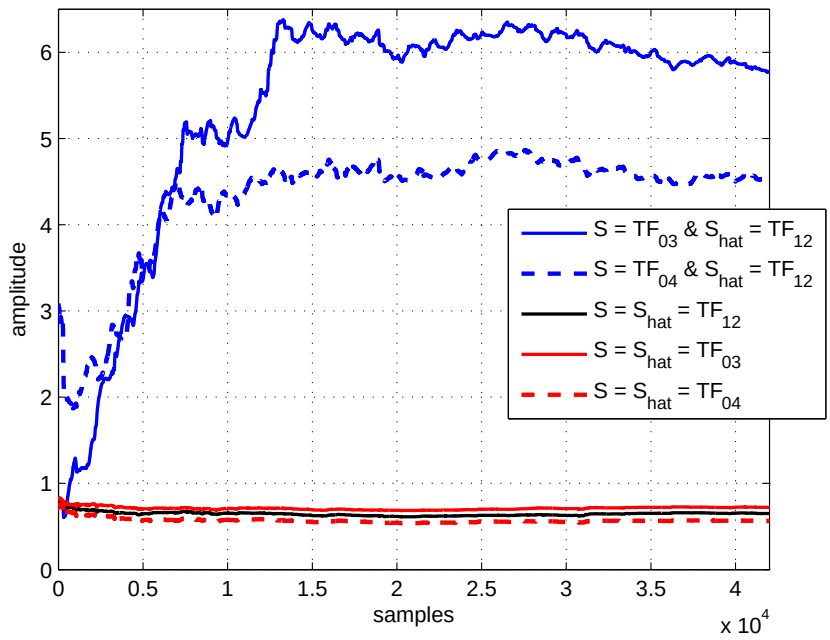

Figure 26: Referenced error signals when implementing different secondary paths of the second set of curves.

21. The transfer fucntions TF_{01} and TF_{02} do not form part of this set of curves.

5.3 Leaky Integrator

The identification of the secondary path is accomplished by computation of the cross-correlation between the test signal $t_s[n]$ and the residual noise signal with the added test signal $e_{in-ts}[n]$. This is done by building a leaky integrator of the form in Eq. 13, where $cc[n]$ is the cross-correlation value at time n and α is the leakage factor. The latter was set at 0.9999, which means that previous values are given more importance than new ones.

$$cc[n+1] \;=\; (1-\alpha)\cdot t_s[n]\cdot e_{in-ts}[n] \;+\; \alpha\cdot cc[n] \tag{13}$$

The structure used for the following simulations is illustrated in Fig. 23 of this section. By adding the test signal to the anti-noise signal it becomes possible to compute the cross-correlation and thus find the ideal type of transfer function needed for implementing $\hat{S}$. The length of both S and $\hat{S}$ was set at 8192 taps while the step size μ was kept at 0.001.

Illustrated in Fig. 27 is the correlation computed using Eq. 13 for two different choices for $\hat{S}$. The goal here is to simulate a change in the manner of wearing the headphones from a leak-proof into a leaky manner and see the impact on the referenced error signal as well as on the cross-correlation between $t_s[n]$ and $e_{in-ts}[n]$. This is done exemplarely by taking TF_{08}, precisely a transfer function from the first set of curves, for the implementation of S during the first $500ms$ or $22\,050$ samples. The change is done by chosing a transfer function from the second set of curves, in this case TF_{11}, for the rest of the simulation. The sets of curves with their respective correlation gains can be found in Fig. 25.

The cross-correlation should change its course as soon as the secondary path S is changed. Since a tranfer function from the first set of curves (leak-proof group) was taken for the implementation of S_A and thus the computation of the cross-correlation, see Section 5.1, a high correlation value is expected for the first half of the simulations illustrated in Fig. 27. During the second halfs on the other hand, a decreasing cross-correlation is expected given the fact that S has been exchanged to a transfer function from the leaky group of curves.

In the first case where a transfer function from the leak-proof set of curves is chosen for the implementation of $\hat{S}$, i.e. the blue curves in Fig. 27 and Fig. 28, constitutes a good example of how the online secondary path identification method could be used.

The correlation value lies from the $26\,000^{th}$ sample on above -0.001, while the referenced squared error signal is growing but is still in a safe range concerning the algorithm's stability. If one was to set a threshold at -0.001 to detect what is considered to be a leak-proof from a leaky manner of wearing the headphones, it would still be possible to chose another $\hat{S}$ from the other set of curves before letting the referenced squared error signal grow.

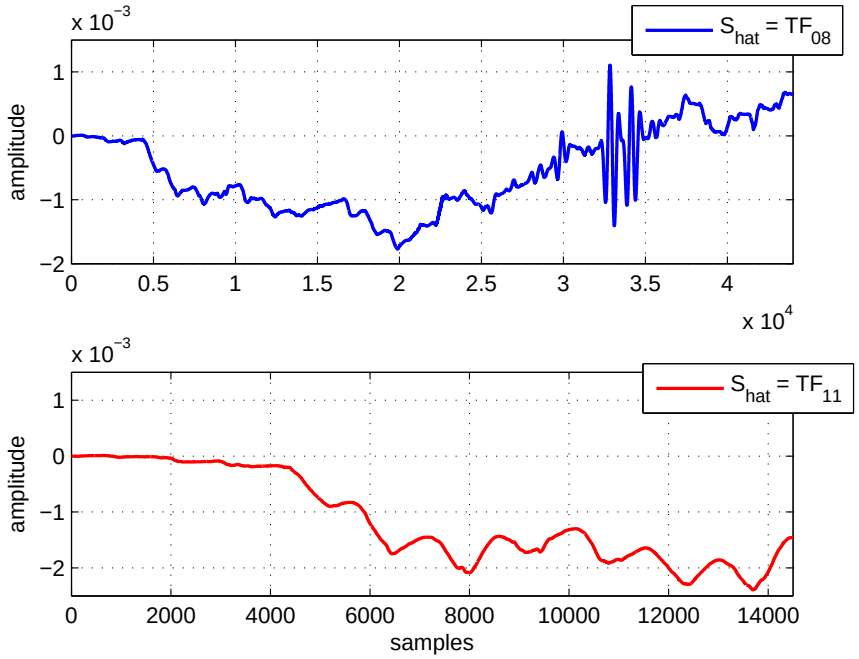

Figure 27: Cross-correlation vector $\mathbf{cc}[n]$ between the test signal $t_s[n]$ and the residual noise signal $e_{in-ts}[n]$.

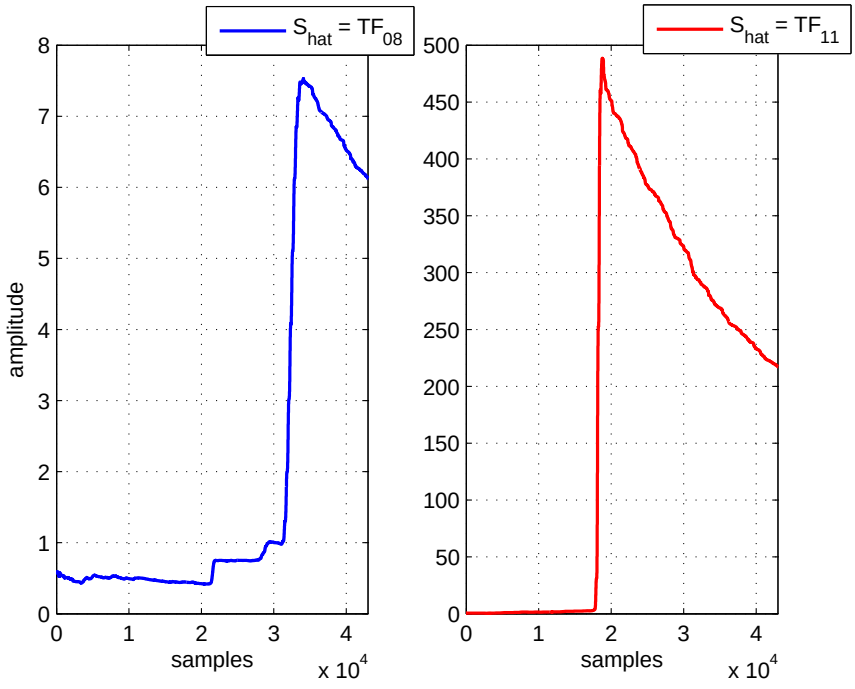

Figure 28: Referenced squared error signals.

Chosing a transfer function for the implementation of $\hat{S}$ from the same set of curves as S means that Eq. 3 is being approximated. The result can be seen in the first half of the simulation where the algorithm works well and as a consequence the referenced squared error signal decreases. Once the secondary path S is modelled by a tranfer function from the leaky group, the referenced error signal begins to grow since $\hat{S}$ is not modelling S accurately enough anymore. The amplitude of the squared error signal also grows pointing to a possible instability.

This could be avoided if a transfer function from the second set of curves had been chosen for $\hat{S}$ once the threshold is surpassed. Why the cross-correlation value of the blue curve in Fig. 27 is still growing at the end of the simulation could be explaind by the excessive amplitude levels of the referenced squared error signal that lead presumably to large correlation values.

Both red curves correspond to the second case where a tranfer function from the leaky set of curves is chosen to model $\hat{S}$. Thus Eq. 3 does not hold during the first half of the simulation, while a high correlation is expected since S_A is still modelled by a transfer function from the leak-proof group of curves. Analogous to the results obtained in Section 3.2.2, the referenced error signal begins to grow immesurably at one point.

A detection of the secondary path S could be possible by setting again the threshold of the cross-correlation at -0.001. The value of the latter passes this threshold from the $6\ 500^{th}$ sample on and stayes in that range. For this case, only the first $14\ 000$ samples were plotted beacause the correlation values begin to burst before half the simulation time for then decrease towards zero. The threshold could not be seen that accurately if all the simulation time was displayed.

All the same, the idea remains as before. The correlation between the test signal and the signal delivered by the inner microphone is growing since the headphones are being worn in a leak-proof manner during the first half of the simulation. This means that the inner microphones are able to measure the test signal and another transfer function, this time from the first set of curves, should be taken for the implementation of $\hat{S}$.

Once S is changed, simulating now a leaky manner of wearing the headphones, the correlation converges towards zero. This is exactly what is expected since there is no significant statistical relationship between the test signal and any of the transfer functions of the leaky set of curves. In order for the algorithm to remain stable, a change in the implementation of $\hat{S}$ has to take place early enough, eventually before the $13\ 000^{th}$ sample already, thus before the referenced error signal bursts.

For this particular simulation, a threshold of -0.001 could be identified for both cases. If a curve from the leak-proof group of curves is taken for the implementation of $\hat{S}$, then a change to a transfer function from the leaky group should take place as soon as

the cross-correlation value goes thorugh the threshold towards zero. Meaning there has been a change in the manner of wearing the headphones pointing to a possible air leakage.

On the other hand, once a transfer function from the second set of curves has been chosen to describe $\hat{S}$, a change to another transfer function from the first set of curves should be carried out as soon as the cross-correlation value exceeds the threshold. This would mean that the headphones are being worn in a leak-proof manner and that $\hat{S}$ does not match the secondary path.

With these results, it has been shown how the online secondary path identification method could be used. Further simulations would be necessary, with other disturbing signals and settings amongst others, in order to assure a correct succession of the method as well as a more profound analysis in order to evaluate the amelioration of the algorithm's performances.

6 Resume and Outlook

A wide variety of simulations were done within the framework of this project. Different structures for the LMS algorithm were implemented while varying relevant parameters such as the step size μ, the system's latency Δt or even the accuracy employed for the secondary path's estimation. The algorithm's performance and stability criteria were analysed in an attempt to understand and comply the ANC system's necessities.

As it turned out, the system's stability is extremely sensitive when making use of the $Feedback$ structure of the LMS algorithm, see Section 3.2. In order to estimate the disturbing signal $x[n]$, the secondary path's estimation $\hat{S}$ is needed, as seen in Fig. 2, one additional time. The influence of $\hat{S}$ is therefore greater than for the $Feedforward$ structure (see also Section 3). An online secondary path identification method is thus necessary when aiming at keeping the algorithm stable or improving its performance. It has been shown that the $Feedback$ implementation of the LMS algorithm becomes unstable once Eq. 3 is not valid and great disparities between S and $\hat{S}$ are given. This when cancelling a broad band signal. The immediate consequence for the ANC system is the inability to cancel the disturbing signal.

With this knowledge an identification method, that relies on a data base of measured secondary paths, has been developed. The main idea is to leak a test signal while the listener is wearing the headphones in order to identify the manner in which they are being worn. This is done as presented in Section 5.1 by computation of the statistical relationship between the test and error signals given by the cross-correlation sequence. The error signal with the added test signal [22] is provided in real time by the inner microphone of the ANC headphones. Is there a large correlation between both signals, then it can be assumed that the headphones are worn in a leak-proof manner. Thus the most adequate transfer function out of the data base can be implemented for describing $\hat{S}$. Is the correlation on the other hand rather low, then the headphones are worn in a somewhat leaky manner and another transfer function, out of another set of curves, can be implemented.

A further step in guaranteeing the algorithm's stability and also improving its performace has been made by means of an online secondary path identification. Its robustness can be increased by characterising the secondary path, i.e. assigning it to one of the two sets of curves proposed in Section 5.2. Hence by choosing the most appropriate transfer function from the data base in order to compensate the ifluence of the secondary path S.

The proposed method has been described and tested to a certain extent. For this specific purpose it seems to work fine and deliver the desired results for facilitating enough information in order to classify the secondary path. Its use in ANC could be of benefit when a $Feedback$ implementation of the LMS algorithm is considered and more robustness concerning its stability is desired.

22. This signal is reproduced by the loudspeakers themselves.

References

[AAK04] M. T. Akhtar, M. Abe, and M. Kawamata, "Modified-filtered-x-lms algorithm based anc systems with improved online secondary path modeling," *The 47th IEEE International Midwest Symposium on Circuits nad Systems*, 2004.

[AM10] M. T. Akhtar and W. Mitsuhashi, "A modified fxlms algorithm for active noise control of impulsive noise," *18th European Signal Processing Conference*, 2010.

[Dou94] S. C. Douglas, "A family of normalized lms algorithms," *IEEE Signal Processing Letters*, vol. SPL-1, no. 3, 1994.

[Goe06] T. Goerne, *Tontechnik*. Fachbuchverlag Leipzig, 2006.

[Gul12] M. Guldenschuh, "Final report of the aap workpackage 2.4 noise cancellation for headphones," 2012.

[Hay02] S. Hayken, *Adaptive Filter Thoery*, 4th ed. Prentice-Hall Inc., 2002.

[KM99] S. M. Kuo and D. R. Morgan, "Active noise control: A tutorial review," vol. 87, no. 6, 1999.

[LP02] P. A. C. Lopes and M. S. Piedade, "The behavior of the modified fxlms algorithm with secondary path modelling errors," *IEEE Signal Processing Letters*, vol. 1, no. 8, 2002.

[Mor80] D. R. Morgan, "An analysis of multiple correlation cancellation loops with a filter in the auxiliary path," *IEEE Trans. Acoust.*, vol. ASSP-28, 1980.

[RS96] M. Rupp and A. H. Sayed, "Modified fxlms algorithm with improved convergence performance," *Proceedings of ASILOMAR-29*, 1996.

[SH90] S. D. Snyder and C. H. Hansen, "The influence of transducer transfer functions and acoustic time delays on the implementation of the lms algorithm in anc systems," *Journal Of Sound And Vibration*, 1990.

[SH94] ——, "The effects of transfer function estimation errors on the filtered-x lms algorithm," *IEEE Transactions ON Signal Processing*, vol. 42, no. 4, 1994.

[Tes12] G. Teschinegg, "Digitale aktive geräuschunterdrückung mit geringer latenz," Thesis, Institut für Elektronische Musik und Akustik, Kunstuni Graz, Technical University Graz, Graz, A, 2012.

[WH60] B. Widrow and M. Hoff, "Adaptive switching circuits," *IRE WESCON Convention Record, pp.96-104*, 1960.

[ZLS01] M. Zhang, H. Lan, and W. Ser, "Cross-updated active noise control system with online secondary path modeling," *IEEE Transactions On Speech And Audio Processing*, vol. 9, no. 5, 2001.